AD-A034 824 COLD REGIONS RESEARCH AND ENGINEERING LAB HANOVER N H F/G 8/7
TOPOLOGICAL PROPERTIES OF SOME TRELLIS PATTERN CHANNEL NETWORKS--ETC(U)
DEC 76 S J MOCK

UNCLASSIFIED CRREL-76-46 NL

1 OF 1
AD A034824

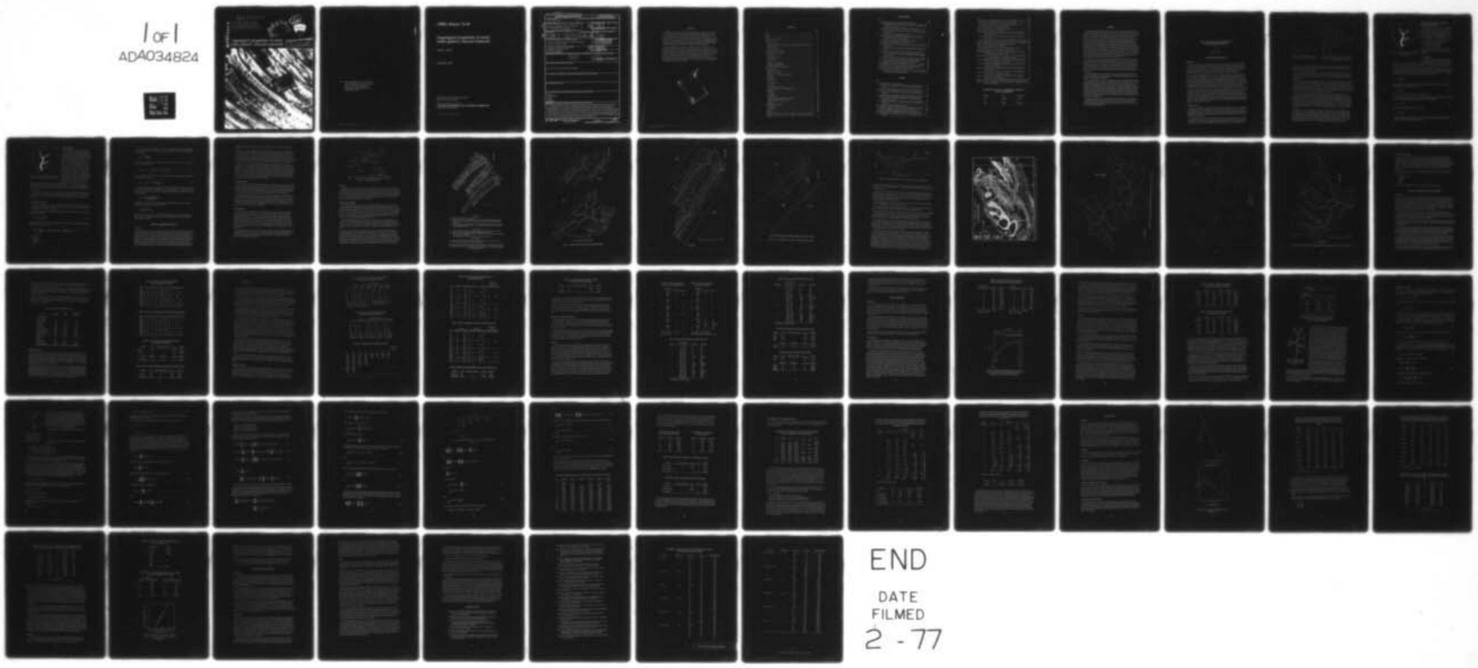

END

DATE
FILMED
2 - 77

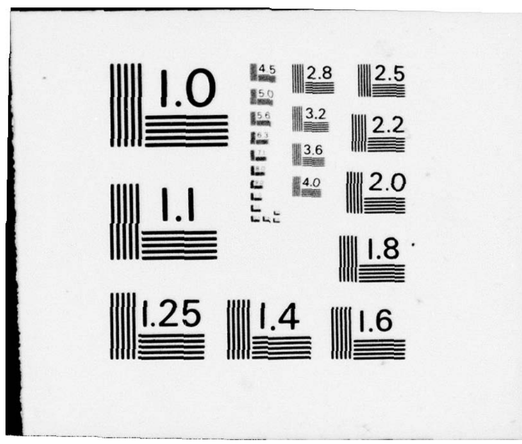
1.0
1.1
1.25
1.4
1.6
1.8
2.0
2.2
2.5
2.8
3.2
3.6
4.0
4.5
5.0
5.6
6.3

CRREL

REPORT 76-46

CRREL

Topological properties of some trellis pattern channel networks

Cover: The ridge and valley section of central Pennsylvania from 50,000 feet. Trellis pattern stream networks are classically developed here. (Photograph by National Aeronautics and Space Administration.)

CRREL Report 76-46

Topological properties of some trellis pattern channel networks

Steven J. Mock

December 1976

Prepared for
DIRECTORATE OF FACILITIES ENGINEERING
OFFICE, CHIEF OF ENGINEERS
By
CORPS OF ENGINEERS, U.S. ARMY
COLD REGIONS RESEARCH AND ENGINEERING LABORATORY
HANOVER, NEW HAMPSHIRE

Unclassified

SECURITY CLASSIFICATION OF THIS PAGE (When Data Entered)

REPORT DOCUMENTATION PAGE

READ INSTRUCTIONS BEFORE COMPLETING FORM

1. REPORT NUMBER: CRREL Report 76-46	2. GOVT ACCESSION NO.
3. RECIPIENT'S CATALOG NUMBER	
4. TITLE (and Subtitle): (6) TOPOLOGICAL PROPERTIES OF SOME TRELLIS PATTERN CHANNEL NETWORKS.	5. TYPE OF REPORT & PERIOD COVERED: (12) 59p.
	6. PERFORMING ORG. REPORT NUMBER
7. AUTHOR(s): (10) Steven J. Mock (14) CRREL-76-46	8. CONTRACT OR GRANT NUMBER(s) (16)
9. PERFORMING ORGANIZATION NAME AND ADDRESS: U.S. Army Cold Regions Research and Engineering Laboratory, Hanover, New Hampshire 03755	10. PROGRAM ELEMENT, PROJECT, TASK AREA & WORK UNIT NUMBERS: DA Project 4A161102AT24, Task Area A2, Work Unit 001
11. CONTROLLING OFFICE NAME AND ADDRESS: Directorate of Facilities Engineering, Office, Chief of Engineers, Washington, D.C. 20314	12. REPORT DATE: (11) December 1976
	13. NUMBER OF PAGES: 59
14. MONITORING AGENCY NAME & ADDRESS (if different from Controlling Office): (17) A2	15. SECURITY CLASS. (of this report): Unclassified
	15a. DECLASSIFICATION/DOWNGRADING SCHEDULE

16. DISTRIBUTION STATEMENT (of this Report)

Approved for public release; distribution unlimited.

17. DISTRIBUTION STATEMENT (of the abstract entered in Block 20, if different from Report)

18. SUPPLEMENTARY NOTES

19. KEY WORDS (Continue on reverse side if necessary and identify by block number)

Geology
Geomorphology
Streams
Topology
Watersheds

20. ABSTRACT (Continue on reverse side if necessary and identify by block number)

The topological properties of 10 stream networks having moderate to well developed trellis drainage patterns have been compared with those expected in a topologically random population. Magnitude 4 subnetworks show a systematic departure from expectation which can be related to geological controls. A link type classification system was developed and a series of equations describing the probability of occurrence of link types in topologically random populations derived. Analysis of the link structure in the channel networks showed small but persistent deviations from expectation in the well developed trellis pattern streams. The general conclusion is that the topologically random model is a very useful standard with which to compare real channel networks.

DD FORM 1 JAN 73 1473 EDITION OF 1 NOV 65 IS OBSOLETE

037100

Unclassified

SECURITY CLASSIFICATION OF THIS PAGE (When Data Entered)

PREFACE

This report was prepared by Dr. Steven J. Mock, Research Geologist, Snow and Ice Branch, Research Division, U.S. Army Cold Regions Research and Engineering Laboratory. It was submitted to the Department of Geology, Northwestern University, in partial fulfillment of the requirements for the degree of Doctor of Philosophy in the field of geology. The work was funded under DA Project 4A161102AT24, ***Research in Snow,*** *Ice and Frozen Ground*, Task Area A2, *Cold Regions Environmental Interactions*, Work Unit 001, *Quantification of Cold Regions Terrain and Climatic Parameters.*

The author would like to express sincere appreciation to Dr. W.F. Weeks, Dr. C.C. Langway, Jr., and Dr. K.F. Sterrett, who provided continual encouragement prior to and throughout the project. Professor W.C. Krumbein of Northwestern University introduced the author to the subject of channel network topology and encouraged him to explore it further. The author would also like to acknowledge the assistance of the CRREL drafting section under H. Larsen, and in particular M. Pacillo who undertook the task of preparing the final channel network maps. Technical review of the report was performed by Dr. Weeks and S.F. Ackley of CRREL.

CONTENTS

ILLUSTRATIONS

TABLES

CONVERSION FACTORS: U.S. CUSTOMARY TO METRIC (SI) UNITS OF MEASUREMENT

Multiply	*By*	*To obtain*
foot	0.3048	meter
mile	1.6093	kilometer

SUMMARY

The topological properties of ten stream networks have been analyzed and compared with those predicted by the topologically random model. The topologically random model states that, in the absence of geological controls, all topologically distinct channel networks having the same number of sources are equally likely, and, in an infinite topologically random network, all topologically distinct sub-networks occur with equal frequency. The ten stream networks have moderately- to well-developed trellis drainage patterns which have formed in response to differential erosion acting on sequences of folded and tilted sedimentary rocks. Testing procedures included examining the frequency of occurrence of topologically distinct channel networks, ambilateral classes and sets of Strahler stream numbers for sub-networks up to magnitude 10. Deviations from predictions of the topologically random model occur in the magnitude-4 networks and are attributed to preferential development of minor tributaries flowing in the down-dip direction of the local rocks. The only other deviation from predicted frequencies occurs in the magnitude-10 stream number sets and is not obviously explicable as a response to geologic controls.

To examine the stream networks in greater detail, a system was devised for classifying individual links by type. Six link types were defined: two exterior types, the T-link and TS-link; and four interior types, the CT-link, B-link, TB-link and T-link. Link types were defined by the magnitude relationships with adjoining links at a link's upstream and downstream terminating forks. Analysis of the link structure shows a greater than expected number of low magnitude T- and TB-links occurring in the sample having a well developed trellis pattern.

The observed departures from the expectations of a topologically random model are related to geological factors, but the deviations are subtle and not observed in the streams having less well developed trellis patterns.

The use of magnitude as a measure of channel network size has great potential, enabling direct comparison of various streams from remotely sensed data or maps. Furthermore, in the absence of gage data, the relative flood potential at any point along a stream can be assessed simply from the growth rate of the magnitude of the main channel up to that point. The fact that trellis patterns deviate only marginally from topological randomness implies that flood hazards within such systems are more or less similar to those within the more common dendritic systems. This information enables assessment of river barrier crossing and denial to be estimated without recourse to long-term flood records which generally are not available at specific sites.

The general conclusion is that the topologically random model serves as a very useful standard with which to compare real channel networks. Furthermore, the presence of strong geological controls, which affect the channel network patterns, has only minor effects on the topological properties.

TOPOLOGICAL PROPERTIES OF SOME TRELLIS PATTERN CHANNEL NETWORKS

by

Steven J. Mock

BACKGROUND AND OBJECTIVES

Introduction

The study of streams and stream networks from a geomorphological rather than a hydrological viewpoint has encompassed three clear and distinct eras, each of which can be associated with one or two dominating individuals. The first era was largely given to descriptive work, the elucidation of a stream's age and place in the erosion cycle by observation and inductive reasoning. The culmination of this era was reached in the many works of W.M. Davis and D. Johnson.

The second era was inaugurated by Robert Horton's work (1932, 1945) and culminated in the studies of Strahler and his students. Horton's major contribution was in devising a methodical system of describing networks numerically, thus allowing statistical analysis and comparative studies of stream systems. Under Strahler's impetus, stream basin parameters were devised and quantified, and the interrelationships among parameters were sought by statistical techniques. Extensive studies of drainage basins have led to the exposition of several "laws" relating various stream and basin parameters. Many of his techniques, including the stream ordering system, are in standard use today.

The third period began with R.L. Shreve's publications of 1966 and 1967 in which he examined the network structure of stream systems from a topological point of view. Once a single basic assumption was made, several of the empirical laws then became derivable as maximum-likelihood events. The concepts of magnitude and links were introduced, and these focused attention on what now seems to be a fundamental element in stream networks. A fusion of elements from the Horton-Strahler "school" with the newer topological view is now in progress, promising and delivering basic insights into the makeup of streams.

Objective of study

The infinite, topologically random model as stated by Shreve (1966, p. 27) is "...in the absence of geologic controls a natural population of channel networks will be topologically random," and later (Shreve 1967, p. 178) "...in the overall network which will be termed an infinite topologically random channel network, all topologically distinct sub-networks with the same number of sources occur with equal frequency."

Topological identity means that the planimetric projections of two channel networks with the same number of sources can be rotated and deformed within the projection plane so as to become congruent. Figure 1 illustrates topological identity and distinction. Only two properties are

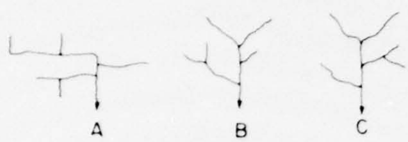

Figure 1. Topologically identical (A and B) and distinct (C) channel networks.

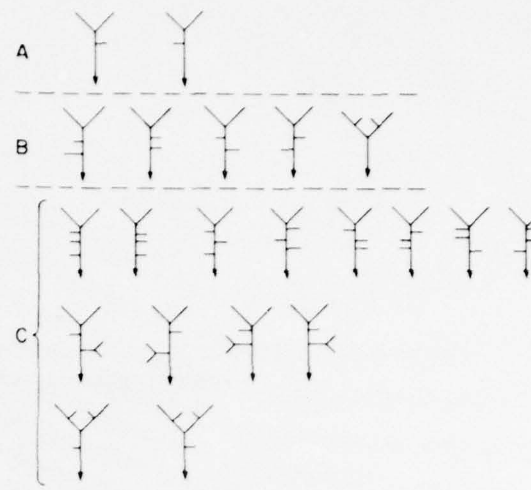

Figure 2. All topologically distinct arrangements for magnitude-3 (A), magnitude-4 (B) and magnitude-5 (C) networks.

necessary to define topological identity — the number of sources, and the arrangement by which they are linked together to form a network. Most of the common geomorphic descriptors and parameters are independent of topology.

Figure 2 shows the topologically distinct arrangements possible for three different size networks. While it is obvious from Figure 2 that the number of topologically distinct arrangements increases rapidly with increasing network size, a specific expression for that number will be postponed until a later section.

Since Shreve introduced the topologically random model, a sizable body of work has accumulated in which natural channel networks have been examined within the predictive framework of the model. For the most part, Smart (1969) being an exception, such studies have examined natural networks which have evidence of minimal geologic control in the channel network development. Channel networks developed on horizontal or gently dipping rocks with homogeneous lithologies and displaying the classical pattern have formed the dominant subject material.

In this study, the topologic properties of 10 channel networks, all showing clear evidence of geologic control, are compared with those predicted by topologically random models. If it can be demonstrated that a correlation exists between geological structure and topological properties then a new method of examining the interaction of geology and streams is available which may provide insights into the evolution and subsequent readjustments within the system. Conversely, if no such correlation can be shown, then there is legitimate reason for broadening the scope of the topologically random model by deleting "...in the absence of geologic controls..." from Shreve's original statement.

In order to carry out the comparison cited above, several new methods of describing channel networks and their component parts are developed. Each of these is shown as being predictable, in a probabilistic sense, from the topologically random model. In particular, a small set of definable sub-units or links are defined with which an entire channel network can be described. While these link types are defined on the basis of numerical relationships with other links at junctions, evidence indicates that each of the link types has distinct length-frequency distributions.

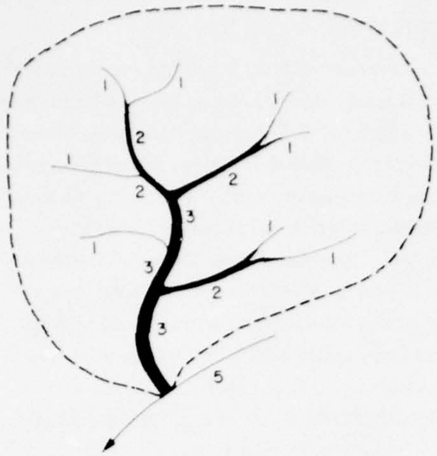

Figure 3. A channel network illustrating the Strahler ordering system.

Quantitative geomorphology and the infinite topologically random model

Horton (1945) can fairly be said to have supplied the foundations for what has since become known as quantitative geomorphology. While Horton's work considered the morphological development of the entire drainage basin, three important aspects of the study deal only with channel networks:

1. Development of a numerical method (stream order) for describing a channel network.
2. The law of stream numbers.
3. The law of stream lengths.

Subsequently, the ordering system was modified slightly by Strahler (1952). The Strahler system is used here.

Stream ordering

The ultimate tributaries in a channel network are designated as order 1. Wherever two streams of the same order, Ω, join, the resulting stream is of order $\Omega+1$. Wherever two streams of unequal order join, the succeeding streams are of the higher order. Figure 3 illustrates the ordering system.

A complete stream consists of the entire reach of channels from the formation of order Ω to the point where it terminates in a higher order. Thus in Figure 3 there are eight 1st order streams, three 2nd order streams, and one 3rd order stream. If we let N_Ω and $N_{\Omega+1}$ be the number of streams of order Ω and $\Omega+1$ respectively, then R_b, the bifurcation ratio, is defined as

$$R_b = \frac{N_\Omega}{N_{\Omega+1}} . \tag{1}$$

The empirical fact that R_b tends towards a constant through a range of Ω's led Horton (1945) to formulate the law of stream numbers, namely:

$$N_\Omega = R_b^{k-\Omega} \tag{2}$$

where k is the order of the master stream (or drainage basin).

One would intuitively expect that on the average the mean length of streams would increase with order. Based on observed data, Horton stated the law of stream lengths:

$$\overline{L}_\Omega = L_1 R_L^{\Omega-1} \tag{3}$$

where $\overline{L}_\Omega$ is the mean length of Ω order streams and

$$R_L = \frac{\overline{L}_\Omega}{\overline{L}_{\Omega-1}} .$$

While both eq 2 and 3 have been found to be valid in many studies, it should be remembered that they are empirical laws based on observation.

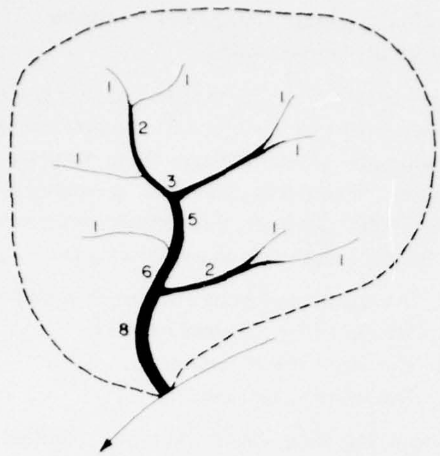

Figure 4. The same channel network as shown in Figure 3, illustrating the magnitude system.

Stream magnitude

Shreve (1967) introduced the concept of stream magnitude. However, before magnitude can be defined, it is necessary to define certain other items. Shreve (1966, p. 20) defined terms in the following manner: "The points farthest upstream in a channel network are termed *sources*. The point of confluence of two channels is a *fork*. The term *link* will refer to a section of channel reaching without intervening forks from either a fork or a source at its upstream end to either a fork or the outlet at its downstream end." Links may be subdivided into *exterior* links, which head at a source, and *interior* links, which head at a fork (Shreve 1967). The *magnitude of a link* "is equal to the total number of sources ultimately tributary to it" (Shreve 1967, p. 179) where all sources are assigned a magnitude of 1. Magnitude is an additive property; two links joining at a fork produce a third link whose magnitude is the sum of the magnitudes of the first two. The *magnitude of a stream network* is defined as being equal to the magnitude of the outlet link, which is defined by the investigator.

Figure 4 shows the same drainage basin as in Figure 3 but now with each link assigned a magnitude according to the above stated rules. Two items worth noting here are 1) 1st order streams and magnitude-1 links are equivalent, and 2) the focus shifts from streams to links as basic entities in the system.

Basic properties of networks

Let M signify the magnitude of a network, and μ the magnitude of individual links. A network of magnitude M contains M exterior links ($\mu = 1$) and $M-1$ interior ($\mu > 1$) links. The total number of links is $2M-1$ for a network of magnitude M.

Let $N(M)$ be the number of topologically distinct arrangements possible for a network of magnitude M. $N(M)$ is given by

$$N(M) = \frac{1}{2M-1} \binom{2M-1}{M} \tag{4}$$

(Shreve 1966, p. 29). The number of topologically distinct networks of order Ω having a magnitude of M (Shreve 1966, p. 29) is given by

$$N(M;\Omega) = \sum_{i=1}^{M-1} \left[N(i;\Omega-1) \times N(M-i;\Omega-1) + 2N(i;\Omega) \times \sum_{\omega=1}^{\Omega-1} N(M-i;\omega)\right] \tag{5}$$

$N(1;1) = 1$
$N(1;\Omega) = 0$
$\Omega = 2, 3, \ldots,$
$N(M;1) = 0$
$M \geq 2.$

In a topologically random population of networks of magnitude M, in which all topologically distinct arrangements occur with equal frequency, the probability of occurrence of any particular order is given by

$$P(M;\Omega) = \frac{N(M;\Omega)}{N(M)} \quad . \tag{6}$$

The number of topologically distinct networks of order Ω having $n_1, n_2, ..., n_{\Omega-1}$, 1 streams of order 1, 2, ..., Ω is given by

$$N(n_1, n_2, ..., n_\Omega, 1) = \prod_{\omega=1}^{\Omega-1} 2^{(n_\omega - 2n_{\omega+1})} \binom{n_\omega - 2}{n_\omega - 2n_{\omega+1}} \tag{7}$$

and the probability of occurrence of any set of stream numbers in a topologically random population of magnitude $M(M = n_1)$ is

$$P(n_1, n_2, ..., n_\Omega, 1) = \frac{N(n_1, n_2, ..., n_\Omega, 1)}{N(M)} \quad . \tag{8}$$

An infinite topologically random network is a network of infinite size in which all topologically distinct subnetworks of the same magnitude occur with equal frequency. The probability of drawing a link of magnitude μ at random from a topologically random population of networks of magnitude M is given by

$$\omega(\mu; M) = \frac{(M-\mu+1)N(M-\mu+1)N(\mu)}{(2M-1)N(M)} \tag{9}$$

and as M goes to ∞, it becomes an infinite topologically random network and the probability of drawing a link of magnitude μ at random becomes

$$\nu(\mu) = \frac{2^{-(2\mu-1)}}{2\mu-1} \binom{2\mu-1}{\mu} \tag{10}$$

(Shreve 1967, p. 181). Equations 9 and 10 will be used extensively in a later chapter when link types are studied. Details of the derivation of eq 4-10 may be found in the series of papers by Shreve (1966, 1967, 1969).

CHANNEL NETWORKS AND GEOLOGY

Introduction

A channel network is a complex and dynamic response to climatic and geological factors. If one accepts an equilibrium point of view, both the network and the individual channels adjust to minimize the amount of work necessary to transport the products of erosion. Because of constant changes in the system, a quasi-equilibrium condition prevails. Because actual drainage patterns and hillslopes are quite well adjusted in form and pattern for handling erosional products under many different environments, the implication is that readjustment to radically changed conditions is relatively rapid (Leopold et al. 1964). Geologists and geomorphologists have implicitly assumed that certain patterns manifested by channel networks reflect a degree of equilibrium between the

network and the underlying geology, and have long made use of this as an aid in interpreting geology.

The geometric patterns displayed in plan view (either on maps or aerial or space photos) have been classified by various authorities into anywhere from seven (Zernitz 1932) to eleven (Feldman et al. 1968) major types. In terms of the equilibrium concepts discussed above, several of the major drainage-pattern types (dendritic, trellis, rectangular, annular) can be considered products of an equilibrium adjustment of the streams to the geology. Other types, however, such as a deranged pattern, are not in equilibrium and are the result of recent (in geologic time) catastrophic events.

Fundamental to the relationship between drainage patterns and geology is the concept of differential erosion, which assumes that channels will tend to develop preferentially along lines of least resistance. The principal geological element giving rise to differential resistance to weathering and erosion is lithology. While structural features per se, such as joint systems or fault traces, are also zones of weakness which can and do control stream patterns, the primary influence of geologic structures is in making a variety of lithologies, having differing resistances to erosion, available to erosion. The drainage patterns which develop though are far more diagnostic of the underlying structural features than they are of particular lithologies.

The dendritic pattern

Zernitz (1932) stated that the "dendritic drainage pattern is characterized by irregular branching in all directions with the tributaries joining at all angles." In fact, such a pattern is more in accord with what is generally considered an insequent pattern, which is normally taken to mean a patternless system (Lattman 1968). The dendritic pattern is usually taken to mean a pattern which has the familiar tree-like appearance with random branching and non-random junction angles.

The dendritic pattern characteristically occurs where there is homogeneity in bedrock resistance to erosion. While such a pattern can develop over complexly deformed crystalline rocks, where sedimentary rocks form the bedrock, the dendritic pattern is usually indicative of, at most, gentle tilting such that a widespread lateral homogeneity in lithology exists. Thus, although a gentle tilt on a regional scale may impart a generalized preferred direction of flow, lateral homogeneity in resistance to erosion should allow random branching.

The trellis pattern

The trellis pattern is characterized by one dominant stream direction with a near-orthogonal direction along which major streams are connected and minor tributaries formed. The major geological requirement for the development of trellis patterns is parallel or sub-parallel zones having differential resistance to erosion. While purely structural features such as jointing (Thornbury 1954, p. 121) can lead to the development of a trellis pattern, parallel belts of moderately to steeply dipping sedimentary rocks of diverse lithology far more commonly give rise to trellis patterns. The overall linear appearance of trellis drainage patterns is a result of preferential stream development along the more easily eroded rock units and generally reflects the direction of the regional strike.

While the classification of stream patterns is largely a subjective matter, and the gradations which occur between types are subject to varied interpretation, there is no question that the dendritic pattern is indicative of minor geologic control and the trellis pattern is a response to major, and usually easily recognized, geological factors.

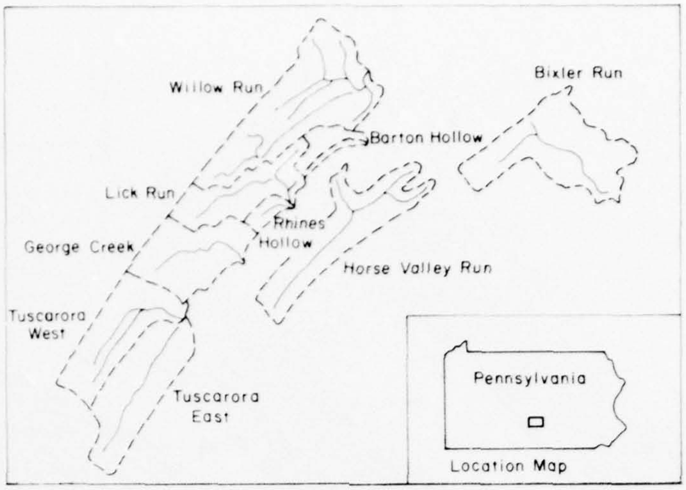

Figure 5. Location map for central Pennsylvania streams. Streams are shown in correct relative positions.

Study areas

Twelve drainage basins were selected for detailed study, nine in central Pennsylvania and three in eastern Pennsylvania and western New Jersey. The basic criterion for selection was that a channel network exhibit a pattern which was clearly a response to geological controls. This in turn dictated that the local geology be known in sufficient detail for identification of at least the major geological controls. Figure 5 shows the location of the central Pennsylvania streams. Figure 9 shows the eastern Pennsylvania and western New Jersey streams.

Geology and physiography

Central Pennsylvania streams. The nine central Pennsylvania streams lie entirely within the Folded Appalachians Physiographic Province (USGS 1970). The area is characterized by a series of alternating and parallel ridges and valleys. Within the study area major ridge crests have an average height of 1900 feet above msl (mean sea level) while the elevation of major valleys is about 600 feet above msl. Secondary ridges and valleys, all paralleling the major relief features, have intermediate elevations. The most distinctive feature of this typical ridge and valley topography is "grain" imparted by the parallelism of the physiographic elements.

Figure 6 is a generalized geologic map of the area in which five of the central Pennsylvania streams are located. The geology shown in Figure 6 is typical of that found throughout this part of Pennsylvania: a Paleozoic sequence of sedimentary rocks with diverse lithologies which has been folded into a series of parallel anticlines and synclines, imparting a regional NE-SW strike to the rocks.

Complete channel networks of the nine central Pennsylvania streams are shown in Figure 7. The drainage patterns are of the classical trellis type. Reference to Figures 6 and 7c, the geologic and channel network maps of the same area, will be useful in understanding the way in which geology has controlled the development of the drainage patterns. The elongated master streams are aligned parallel to the regional strike of rocks while the majority of the lesser tributaries are oriented perpendicular to the master streams and flow up- or down-section, depending upon the local bedrock attitude. The master streams have preferentially developed along zones of weakness which

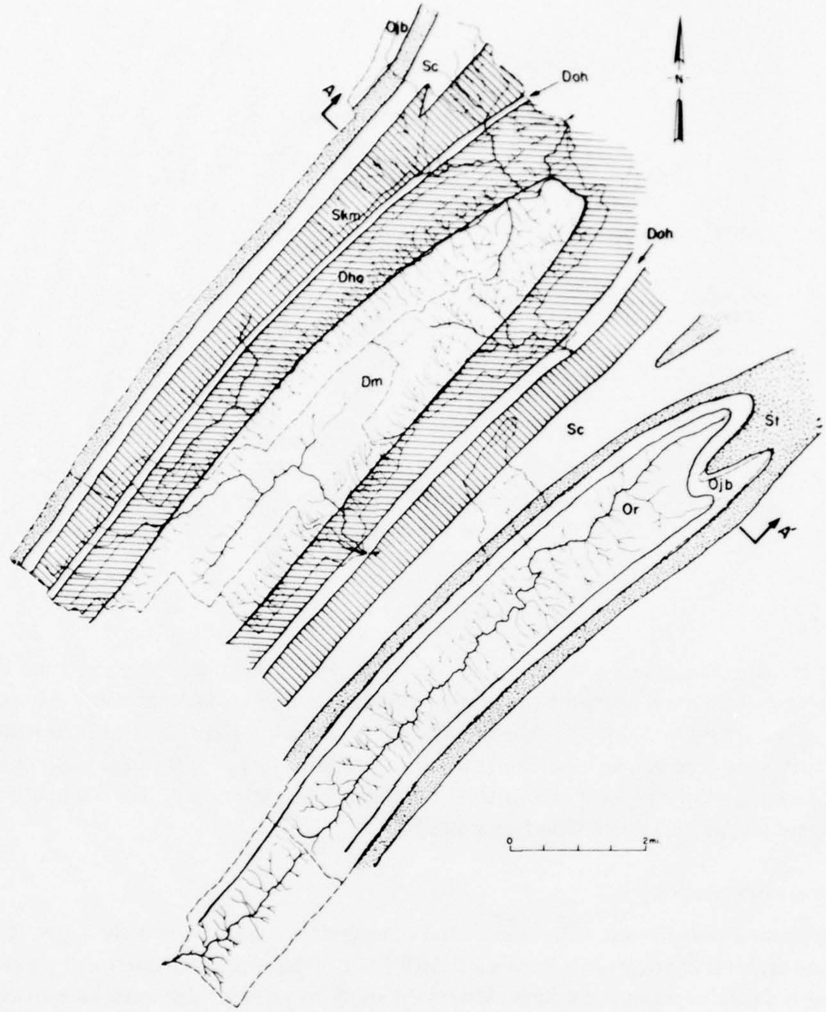

Devonian System

Dm Marine beds: Shales, graywackes and sandstones.

Dho Mahantango – Marcellus – Onandaga Formations, undivided. Shales with interbedded sandstones at bottom, black fissile, carbonaceous shale in middle, and thin bedded shale and medium bedded limestone at top.

Doh Helderberg – Griskany Formations, undivided. Fine to coarse grained sandstone, cherty limestone with some interbedded shales and sandstone at top. Thin bedded shales, cherty limestones to thick bedded crystalline limestone at bottom.

Silurian System

Skm Keyser – Tonoloway – Wills Creek – Bloomsburg – McKenzie Formations, undivided. Limestones grading downward to argillaceous limestones to interbedded shales and limestones.

Sc Clinton Group. Shales, interbedded downward with quartzitic sandstone to thin to medium, bedded shale with intertonguing "iron sandstone."

St Tuscarora Formation. Medium to thick bedded, fine grained, quartzitic sandstone.

Ordovician System

Ojb Juniata – Bald Eagle Formations, undivided. Fine grained to conglomeratic quartzitic sandstones.

Or Reedsville Formation. Shale with thin silty to sandy interbeds.

Figure 6. Generalized geologic map of Willow Run, Barton Hollow, Lick Run, Rhines Hollow and Horse Valley Run. Source: Geologic Map of Pennsylvania (Pennsylvania Geological Survey 1960) and unpublished base maps.

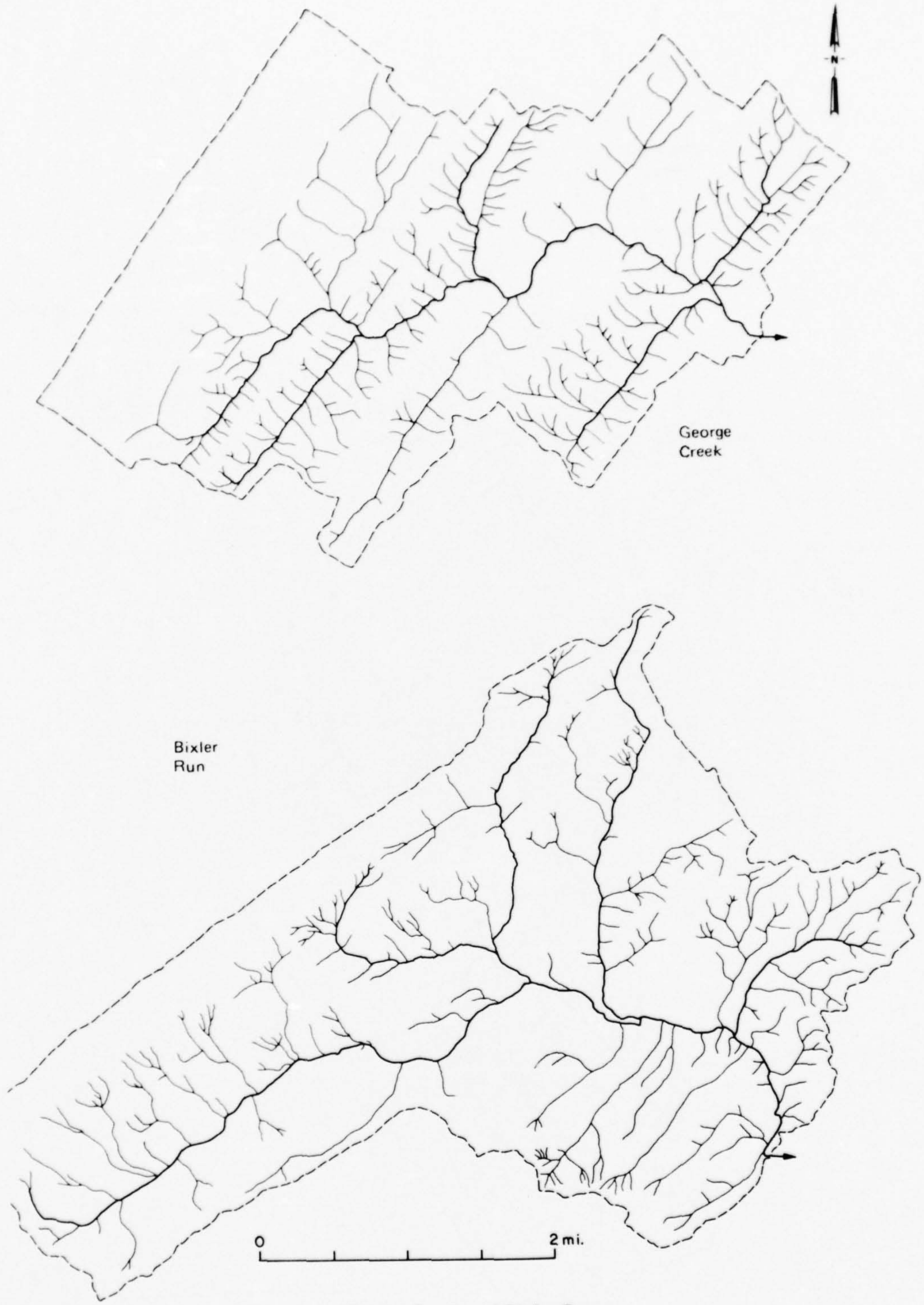

a. George Creek and Bixler Run.

Figure 7. Channel-network maps of central Pennsylvania streams.

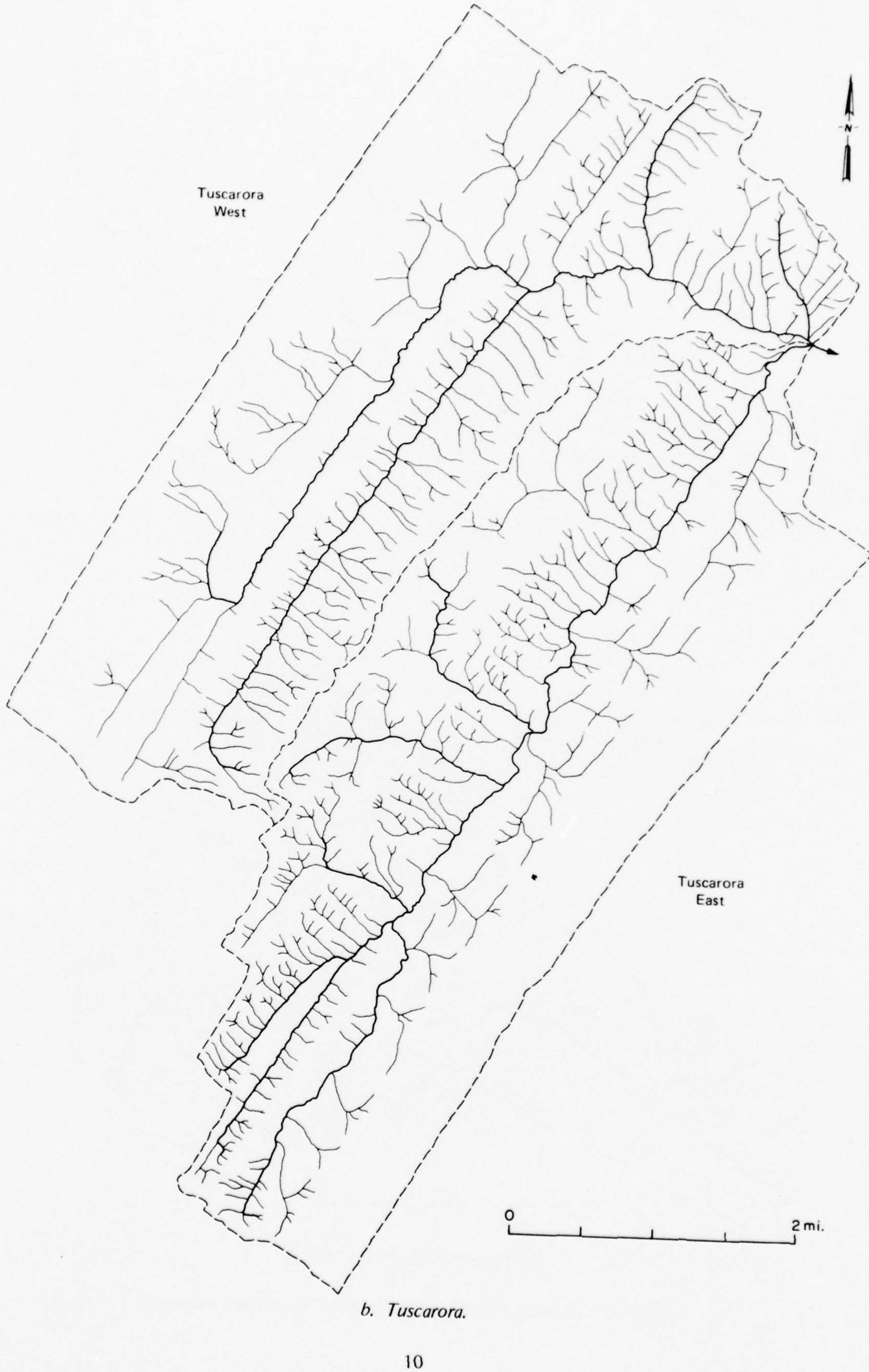

b. Tuscarora.

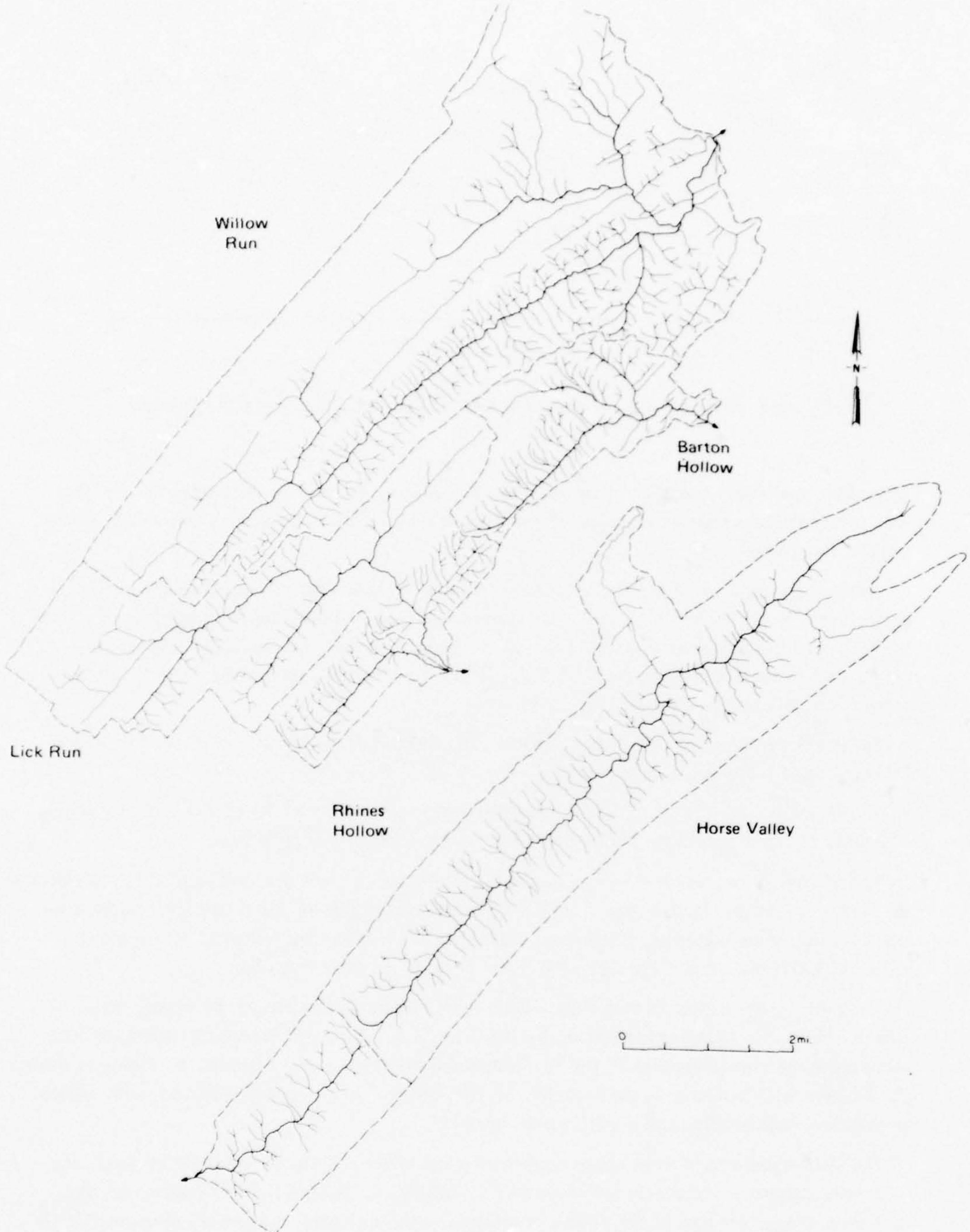

c. Willow Run, Lick Run, Rhines Hollow, Barton Hollow and Horse Valley.

Figure 7 (cont'd). Channel-network maps of central Pennsylvania streams.

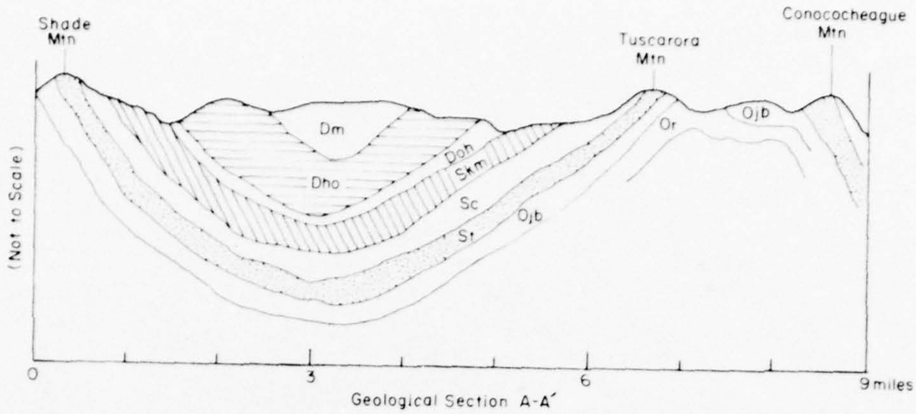

Figure 8. Geologic section along line A-A' of Figure 6. (See Fig. 6 for legend.)

are either more easily eroded rocks or formational contacts. The narrow outcrop pattern of the rock units has caused the development of a series of parallel elongated channels rather than a tree-like channel system.

The present result of differential erosion in this area is a landscape characterized by parallel ridges and valleys. The geologic cross section shown in Figure 8 illustrates the relationship between topography, lithology and structure. The most resistant rock unit, the Tuscarora Formation, a quartzitic sandstone, underlies the three major ridges, while streams are incised into less resistant siltstones, shales and argillaceous limestones.

Eastern Pennsylvania – New Jersey streams. The three drainage basins in this group lie in the Triassic Lowland physiographic province (USGS 1970).

The region and each of the three drainage basins have low to moderate relief with gently rolling hills and occasional steep ridges with local relief on the order of 300 to 400 feet.

The geology of the area is shown in Figure 9 and the channel networks in Figure 10. Geologically, the area is much simpler than that of central Pennsylvania, in that for the most part it can be considered a simple homocline locally interrupted by broad anticlines and synclines. The regional strike is NE-SW with an average regional dip of 15° to 20° to the northwest.

The underlying bedrock in each stream basin is composed of members of the Triassic Newark Group. Three interfingering lithofacies (the Stockton, Lockatong and Brunswick) compose the sedimentary section (Willard et al. 1959). While the lithofacies exhibit a variety of lithologies, each has a dominant one, arkose in the Stockton, argillite in the Lockatong, and shale in the Brunswick. In addition, diabase dikes and sills have been intruded.

The stream patterns in these basins range from moderately well developed trellis to dendritic. The trellis pattern is best developed where the Lockatong and Brunswick lithofacies interfinger, such as in the eastern part of the Tohickon drainage. Streams have preferentially developed in the direction of the regional strike on the less resistant shales of the Brunswick lithofacies. Where lithology becomes more homogeneous, such as the eastern part of the Stony Brook drainage or on the diabase of the Tohickon, a more typical dendritic pattern forms. Despite the less-pronounced development of trellis patterns, the effects of varying resistance to erosion between and within the lithofacies of the Newark Group and the homoclinal structure have enabled differential erosion to develop stream patterns characterized by a moderate degree of parallelism to the regional strike.

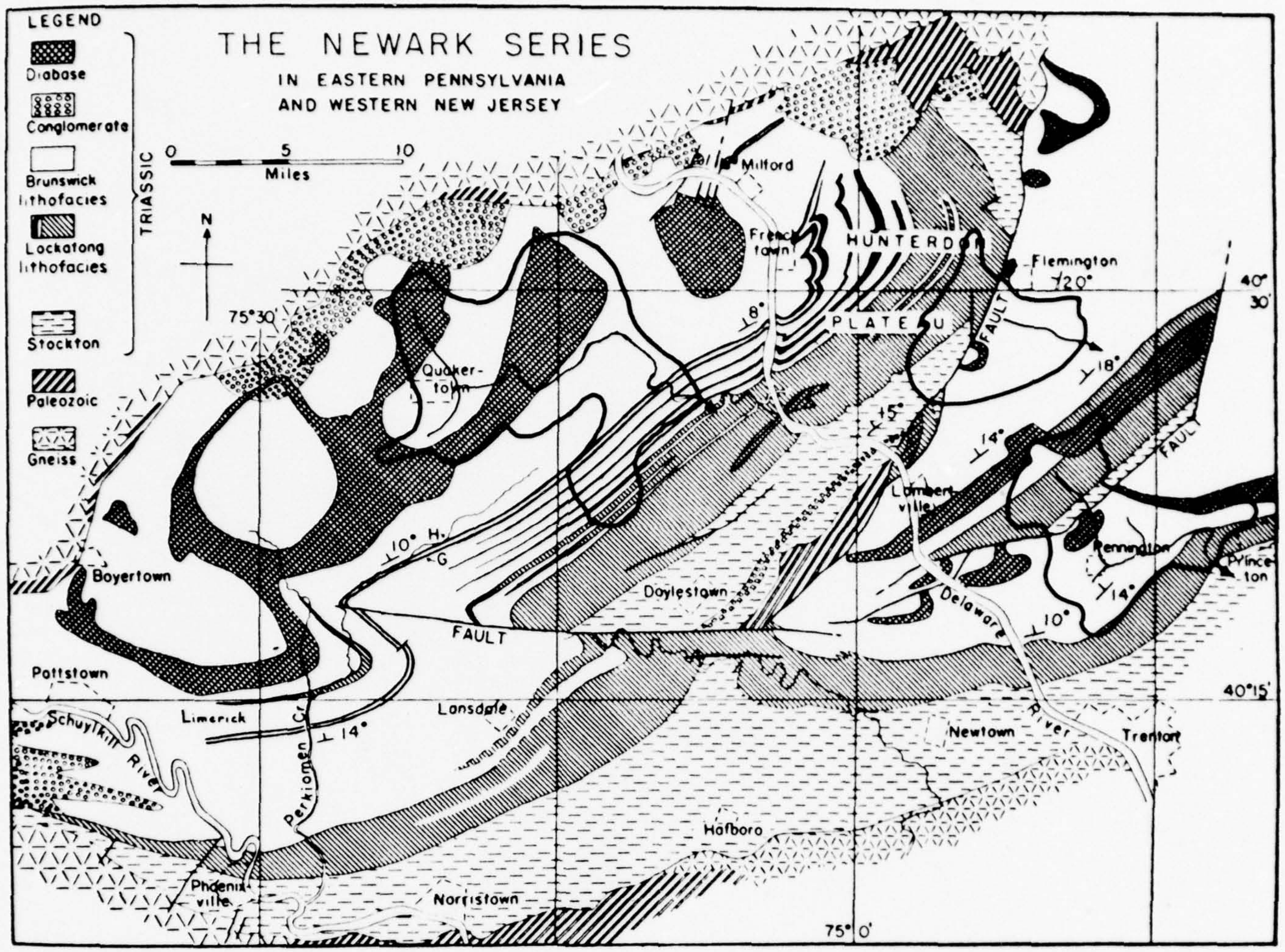

Figure 9. Geologic map of eastern Pennsylvania and western New Jersey with stream basins shown. (Adapted from Willard et al. 1959.)

a. Stony Brook.

Figure 10. Channel network maps of eastern Pennsylvania and western New Jersey streams.

b. *Tohickon Creek.*

Figure 10 (cont'd).

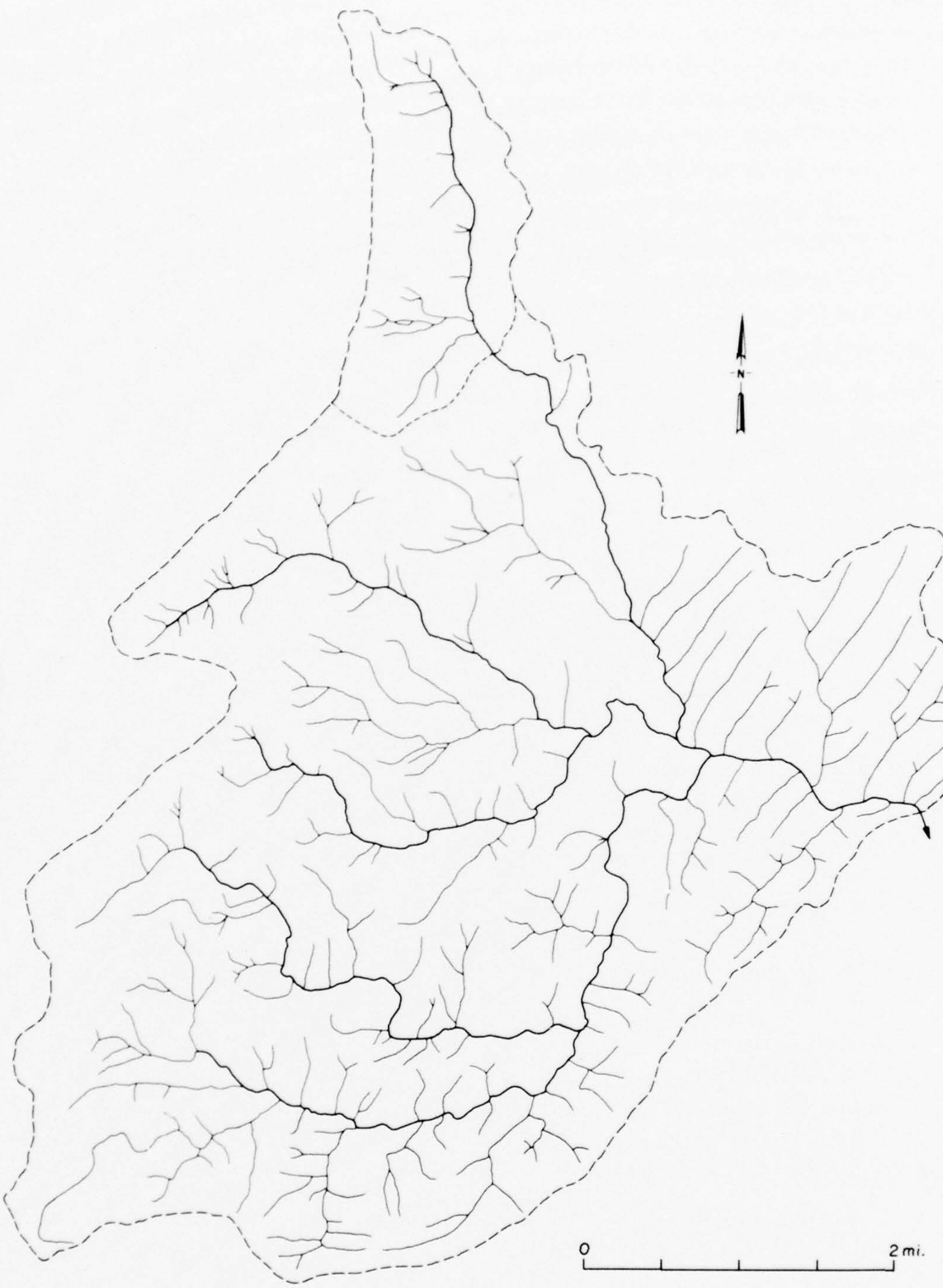

c. Neshanic River.

Figure 10 (cont'd). Channel network maps of eastern Pennsylvania and western New Jersey streams.

Channel network mapping

The channel network of each of the streams was traced in its entirety from 1:24,000 scale topographic maps. Channels not shown as blue lines on the maps were defined by continuous V-shaped contour lines. As a consequence of using contour shape to define channels, an element of operator judgment becomes part of the data. For the most part, this manifests itself in deciding where to terminate a channel as V-shaped contours grade slowly towards U-shaped ones. This problem does not affect topology so much as the study of link lengths, or the measurement of drainage density.

Each link of a channel network was assigned an identification number and the following data were tabulated:

1. Identification number
2. Magnitude
3. Length
4. Type

This information formed the basic data set for much of the subsequent work.

TOPOLOGICAL PROPERTIES OF THE NETWORKS

Introduction

Equation 5 gives the number of topologically distinct channel networks (TDCN) possible for a network of given magnitude. The simplest possible statistical analysis is to test the null hypothesis that TDCN of the same magnitude occur with equal frequency. As a practical matter, this is feasible only with low-magnitude networks because of the rapid increase of $N(M)$ with increasing M and the concomitant difficulty in obtaining a sufficiently large sample. Consequently, it becomes necessary to group TDCN into classes having some common property or, alternatively, to develop other means of classification which can be predicted by the model.

Smart (1968) and Werner and Smart (1973) have reviewed existing methods of topologic classification and have proposed new classification schemes. The general strategy used herein will be to proceed from examining low-magnitude networks to greater-magnitude networks, using at each scale a classification system commensurate with the sample size.

Three methods of classification will be used in addition to TDCN, namely the ambilateral classification introduced by Smart (1969), the right-left classes used by Krumbein and Shreve (1970), and stream number sets.

The following convention will be used in this chapter. Each topologically distinct channel network discussed will be initially illustrated by a schematic channel network map. Associated with a particular TDCN will be a roman numeral, designating the ambilateral class to which it belongs, and one or two letters designating its right-left class. See Table II as an illustration of usage.

The essence of Smart's ambilateral classification is that all TDCN which can be made equivalent by simple right-left reversals at one or more junctions belong to the same ambilateral class. Smart argued that the individual TDCN's within an ambilateral class would be expected to have similar hydrological properties. Furthermore he noted that all TDCN's within an ambilateral class would have the same set of link magnitudes and the same set of stream numbers.

The right-left classification used by Krumbein and Shreve assigns a TDCN to a right or left class based on which side of the main channel (when viewed upstream) has the greatest number of

magnitude-1 streams ultimately tributary to it. In the modified form used herein, TDCN having equal contributions from both sides are classified as rl or lr as shown in Tables II and III.

Stream-number sets are shown in the form $(n_1, n_2, ..., n_{\Omega-1}, 1)$ where n_1 is the number of Strahler first-order streams, n_2 the number of second order streams, etc. Within a topologically random population of given magnitude, the probability of occurrence of each possible stream number set can be calculated from eq 8.

Table I contains basic information for the 12 streams studied here. The first seven streams in Table I are referred to throughout as the contiguous-seven and the last three as the Triassic. For the most part, statistical analysis is confined to these two groups. Complete data for each channel network are given in the Appendix.

Table I. Summary data for stream networks.

Stream	*Magnitude*	*Area (miles^2)*	*Drainage density (mile^{-1})*
Contiguous seven			
Rhines Hollow	51	1.56	7.74
Barton Hollow	102	3.70	7.47
Lick Run	117	9.19	3.83
Willow Run	380	22.84	4.63
George Creek	246	9.49	6.51
Tuscarora Creek E.	385	15.25	5.67
Tuscarora Creek W.	281	13.77	5.32
Horse Valley Run	175	15.24	3.91
Bixler Run	274	15.00	5.06
Triassic			
Neshanic River	259	25.7	4.11
Stony Brook	274	44.5	3.29
Tohickon Creek	311	97.4	2.27

Magnitude-4 networks

There are five topologically distinct arrangements possible for magnitude-4 networks. These arrangements are shown in the first column of Tables II and III. The statistics of magnitude-4 networks for the contiguous-seven and Triassic streams are shown in Tables II and III. In these and later statistical tables, the column headed *Expected* is the expected number of networks which would occur in that particular class for random selection of a sample of size n from a topologically random population of magnitude-M networks.

Statistical analysis of the data is given in Tables IV and V. Throughout the statistical analysis, unless stated otherwise, the null hypothesis tested is: the observed sample data have frequencies of occurrence which could be expected from random selection of an equivalent-size sample from a topologically random population of networks of the particular magnitude under consideration. For samples having three or more classes a chi-square goodness of fit test will be used to decide on acceptance or rejection of the null hypothesis. The generalized likelihood ratio is

Table II. Statistics of the 123 magnitude-4 networks from the contiguous-seven streams.

TDCN	*Class*	*Observed*	*Expected*	*Class*	*Observed*	*Expected*
	Ir	36	24.6	Ir and I	59	49.2
	II	23	24.6			
	IrI	20	24.6	IrI and IIr	37	49.2
	IIr	17	24.6			
	II	27	24.6	II	27	24.6

Table III. Statistics of the 48 magnitude-4 networks from the Triassic streams.

TDCN	*Class*	*Observed*	*Expected*	*Class*	*Observed*	*Expected*
	Ir	10	9.6	Ir and I	19	19.2
	II	9	9.6			
	IrI	5	9.6	IrI and IIr	20	19.2
	IIr	15	9.6			
	II	9	9.6	II	9	9.6

Table IV. Statistical analysis of magnitude-4 networks from the contiguous-seven streams.

Sample	$-2\ln\lambda$	*Degrees of freedom*	$\chi^2_{.05,DF}$	*Decision*
TDCN	8.50	4	9.49	Accept
IrII, IrIIIr, II	5.37	2	5.99	Accept

Sample	*Observed*	*Sample size*	*Crit val*	*Decision*
Ir, II and IrI, IIr	59	96	56	Reject

Table V. Statistical analysis of magnitude-4 networks from the Triassic streams.

Sample	$-2\ln\lambda$	*Degrees of freedom*	$\chi^2_{.05,DF}$	*Decision*
TDCN	5.36	4	9.49	Accept
IrII, IrIIIr, II	0.07	2	5.99	Accept

$$\lambda = n^n \prod_{j=1}^{k+1} \left(\frac{P_j}{n_j}\right)^{n_j}$$

where n is the total sample size, n_j is the number of samples in the j^{th} class of the $k+1$ classes, and P_j is the given or known probability of the j^{th} class (Mood et al. 1974, p. 444). For large values of n, $-2ln\lambda$ has approximately the chi-square distribution with k degrees of freedom, and the decision to reject the null hypothesis is made if $-2ln\lambda > \chi^2_{\alpha,k}$ for the α level of confidence.

In those cases where just two samples are being compared, the binomial distribution is used for testing the null hypothesis. For sample sizes up to 150, tables of the cumulative binomial probabilities were consulted (Army Materiel Command 1972) while for larger sample sizes the normal approximation for the binomial distribution was used (Mood et al. 1974, p. 120-121). For all tests, the decision to accept or reject the null hypothesis was made at the 0.05 level of confidence.

The statistical analysis in Tables IV and V indicates that, with one exception, the null hypothesis can be accepted at the 0.05 significance level. That exception occurs in the comparison of Class Ir and II networks with Class Irl and IIr networks in the contiguous-seven sample. In a topologically random population the two groups occur with equal frequency but the excess of the r and l group over the rl and lr group is sufficiently large to reject the null hypothesis.

The question raised by the excess of the grouped Class Ir and Il channel networks is whether this excess occurs randomly throughout the sample or in some systematic way which can be related to geological or geographical factors. In order to answer this question, the magnitude-4 TDCN's from the contiguous-seven streams were classified as a function of two attributes: 1) direction of flow with respect to local strike, i.e. along-strike or across-strike, and 2) direction of flow with respect to dip, i.e. up- or down-section. The original statement of the topologically random model contains no reference to directional properties of topology. However, "in the absence of geologic controls" implies that the topological properties should be isotropic with respect to geological factors. This in turn means that any subset chosen as a function of a geological characteristic should also be topologically random.

In Tables VI and VII samples from various possible subsets are statistically tested. The null hypothesis in each of these tests is that the sample could have been drawn from a topologically random subset. The results shown in the tables indicate that the null hypothesis can be rejected for the population of networks flowing along-strike. These, of course, are the streams whose tributaries are flowing either up-dip or down-dip to reach the main channel. Of the Class I networks whose tributaries can unambiguously be defined as flowing up- or down-section, approximately 67% have their tributaries flowing down-section, suggesting that this may be the controlling geologic factor.

A similar analysis of the Triassic magnitude-4 networks cannot be made. Orientations of the magnitude-4 networks are less systematic with respect to the bedrock attitude. This, in conjunction with the initially smaller sample, provides a sample size which is too small for meaningful statistical testing.

Magnitude-5 networks

The 14 possible topologically distinct arrangements of a magnitude-5 channel network are shown in Table VIII with right-left and ambilateral classes indicated. Tables IX and X show the statistical analysis. Note that although the observed and expected frequencies of TDCN's are shown in Tables IX and X, no goodness-of-fit tests are given in Tables XI and XII. This illustrates the major difficulties in comparing real channel networks with the topologically random model at the level

Table VI. Direction of flow with respect to regional strike of contiguous-seven magnitude-4 networks.

	Direction of flow					
Class	Along-strike	Across-strike	Inter-mediate	Along-strike	Across-strike	Inter-mediate
Ir Il	15 8	19 14	3 1	23	33	4
Irl Ilr	6 1 } 7*	12 14	2 2	7	26	4
II	9	15	2	9	15	2
$-2ln\lambda$	11.38	1.75		6.43	0.84	
Decision	Reject	Accept		Reject	Accept	

* Combined for goodness-of-fit test.

Table VII. Direction of flow with respect to dip of contiguous-seven magnitude-4 networks.

	Direction of flow			
Class	Down-section	Up-section	Down-section	Up-section
Ir Il	7 9	12 5	16	17
Irl Ilr	3 7	9 7	10	16
II	6	8	6	8
$-2ln\lambda$	3.33	3.26	1.43	0.036
Decision	Accept	Accept	Accept	Accept

Table VIII. Topological classes for magnitude-5 networks.

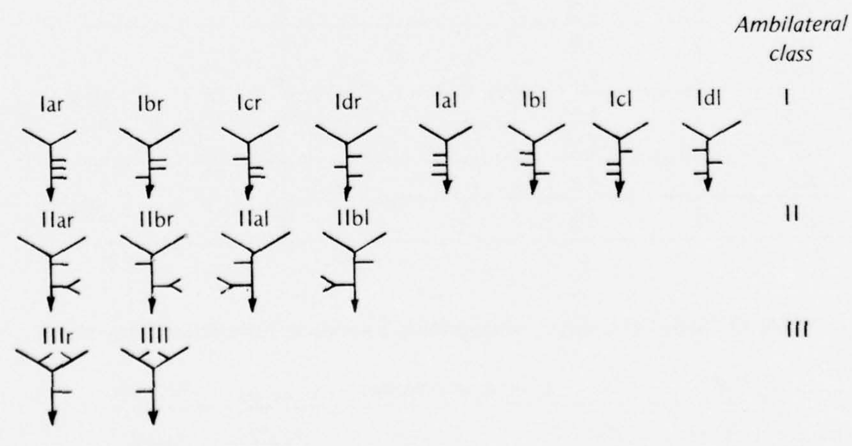

Table IX. Statistics of magnitude-5 networks from the contiguous-seven streams.

Class	Observed	Expected	Observed	Expected	Ambilateral class Observed	Ambilateral class Expected
Iar	12	5.3	22	21.2	43	42.4
Ibr	3	5.3				
Icr	5	5.3				
Idr	2	5.3				
Ial	2	5.3	21	21.2		
Ibl	10	5.3				
Icl	3	5.3				
Idl	6	5.3				
IIar	4	5.3	12	10.6	20	21.2
IIbr	8	5.3				
IIal	2	5.3	8	10.6		
IIbl	6	5.3				
IIIr	6	5.3	6	5.3	11	10.6
IIIl	5	5.3	5	5.3		

Table X. Statistics of magnitude-5 networks from the Triassic streams.

Class	TDCN Observed	TDCN Expected	Right-left Observed	Right-left Expected	Ambilateral class Observed	Ambilateral class Expected
Iar	3	3.2	10	12.8	22	25.6
Ibr	1	3.2				
Icr	4	3.2				
Idr	2	3.2				
Ial	4	3.2	12	12.8		
Ibl	2	3.2				
Icl	2	3.2				
Idl	4	3.2				
IIar	2	3.2	7	6.4	15	12.8
IIbr	5	3.2				
IIal	7	3.2	8	6.4		
IIbl	1	3.2				
IIIr	3	3.2	3	3.2	7	6.4
IIIl	4	3.2	4	3.2		

Table XI. Statistical analysis of magnitude-5 networks from Triassic streams.

Sample	$-2 \ln \lambda$	Degrees of freedom	$\chi^2_{.05, DF}$	Decision
R-L classes	1.33	5	11.07	Accept
Ambilateral	0.97	2	5.99	Accept

Table XII. Statistical analysis of magnitude-5 networks from the contiguous-seven streams.

Sample	*-2lnλ*	*Degrees of freedom*	$\chi^2_{.05,DF}$	*Decision*
R-L classes	1.76	5	11.07	Accept
Ambilateral	0.12	2	5.99	Accept

of TDCN, namely that the number of possible TDCN rises with such rapidity as magnitude increases, that the problem of maintaining a sample size of at least five per class, considered good statistical practice (Miller and Kahn 1962), becomes impractical.

The null hypothesis that these samples could have been drawn from a topologically random population of magnitude-5 networks can be accepted for both samples whether classified by the right-left or the ambilateral system. It is worth noting that the wide disparity between observed and expected TDCN in some classes is completely hidden in the right-left and ambilateral classification.

Magnitude-6 to magnitude-10 networks

The statistics and statistical analyses of magnitude-6 through magnitude-10 streams are shown in Tables XIII-XVIII. For magnitude-6 networks TDCN were grouped according to ambilateral class, while for greater magnitude networks they were combined into stream number sets. Note also that even at the level of stream number sets, it was necessary to combine groups in order to have a satisfactory sample size.

The statistical analysis indicates that, with one exception, there is no reason to reject the hypothesis that these samples were drawn from topologically random populations of the indicated magnitude. That sample for which the null hypothesis can be rejected occurs in the Triassic samples where the stream number set (10, 2, 1) occurs with greater frequency than would be expected in a topologically random population of magnitude-10 networks.

Summary

All channel networks ranging from magnitude 4 to magnitude 10 within the contiguous-seven and Triassic samples have been classified and grouped by TDCN's, right-left classes, ambilateral classes, or stream number sets as appropriate for the available sample size. For each magnitude the null hypothesis that the observed sample could have been drawn from a topologically random population of that magnitude was tested using either a chi-square goodness-of-fit test or a binomial test. The null hypothesis could be rejected at the 0.05 confidence level for two of the samples, that of class I magnitude-4 TDCN's from the contiguous-seven sample and that of magnitude-10 stream number sets from the Triassic sample.

The magnitude-4 networks, for which the null hypothesis could be rejected, were subjected to further study, examining TDCN as function of their flow direction with respect to the attitude of the local bedrock. In so doing it is argued that the topologically random model, in particular the key phrase "in the absence of geologic controls," implies directional isotropy of topology with respect to any geological parameter. Examination of the magnitude-4 streams shows that of those streams which flow in the direction of the local strike, those having tributaries entering from the same side occur with much greater frequency than can be expected in a topologically random population.

Table XIII. Statistics of magnitude-6 networks from the contiguous-seven streams.

	Ambilateral class	Observed	Expected
I		18	20.6
II		6	5.1
III	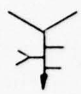	8	10.3
IV	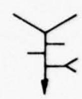	12	10.3
V		4	2.3
VI		6	5.1

$-2 ln\lambda = 2.20$, $\chi^2_{.05, 5} = 11.07$;
Decision: Accept

Table XIV. Statistics of magnitude-6 networks from Triassic streams.

	Ambilateral class	Observed		Expected	
I	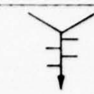	13		13.0	
II		6		3.2	
III		8		6.5	
IV	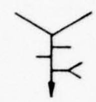	3		6.5	
V	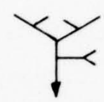	0	4*	1.6	4.8*
VI		4		3.2	

* Combined for statistical testing
$-2 ln\lambda = 8.05$, $\chi^2_{.05, 4} = 9.49$; Decision: Accept

Table XV. Stream-number statistics for the contiguous-seven streams.

Magnitude	Stream numbers (n_1, n_2, n_3, n_4)	Observed		Expected	
	(7, 1, 0, 0)	5		6.5	
7	(7, 2, 1, 0)	19		16.4	
	(7, 3, 1, 0)	3		4.1	
	(8, 1, 0, 0)	4		4.6	
	(8, 2, 1, 0)	18		17.3	
8	(8, 3, 1, 0)	7		8.7	
	(8, 4, 1, 0)	1	2*	0.3	0.4*
	(8, 4, 2, 1)	1		0.1	
	(9, 2, 1, 0)	9		10.8	
	(9, 3, 1, 0)	9		9.0	
9	(9, 4, 1, 0)	1		0.9	
	(9, 4, 2, 1)	2	5*	0.2	3.2*
	(9, 1, 0, 0)	2		2.1	
	(10, 1, 0, 0)	0		1.2	
	(10, 2, 1, 0)	7		8.1	
	(10, 4, 1, 0)	1	9*	2.0	11.8*
10	(10, 4, 2, 1)	1		0.5	
	(10, 5, 1, 0)	0		0.0	
	(10, 5, 2, 1)	0		0.0	
	(10, 3, 1, 0)	13		10.1	

* Combined for statistical testing.

Table XVI. Stream-number statistics for Triassic streams.

Magnitude	Stream numbers (n_1, n_2, n_3, n_4)	Observed		Expected	
	(7, 1, 0, 0)	5		7.0	
7	(7, 2, 1, 0)	22		17.6	
	(7, 3, 1, 0)	2		4.4	
	(8, 2, 1, 0)	16		13.4	
	(8, 1, 0, 0)	2		3.6	
8	(8, 3, 1, 0)	5	7*	6.7	10.6*
	(8, 4, 1, 0)	0		0.2	
	(8, 4, 2, 1)	0		0.1	
	(9, 2, 1, 0)	9		7.5	
	(9, 1, 0, 0)	1		1.4	
9	(9, 3, 1, 0)	5	7*	6.3	8.5*
	(9, 4, 1, 0)	1		0.6	
	(9, 4, 2, 1)	0		0.2	
	(10, 2, 1, 0)	10		5.9	
	(10, 1, 0, 0)	0		0.8	
	(10, 3, 1, 0)	4		7.4	
10	(10, 4, 1, 0)	2	6*	1.5	10.1*
	(10, 4, 2, 1)	0		0.4	
	(10, 5, 1, 0)	0		0.0	
	(10, 5, 2, 1)	0		0.0	

* Combined for statistical testing.

Table XVII. Statistical analysis for contiguous-seven streams.

Sample	$-2 \ln \lambda$	*Degrees of freedom*	$\chi^2_{.05, DF}$	*Decision*
Mag 7	1.11	2	5.99	Accept
Mag 8	4.28	3	7.82	Accept
Mag 9	1.14	2	5.99	Accept

	Observed	*Sample size*	*Crit val*	*Decision*
Mag 10	13	22	15	Accept

Table XVIII. Statistical analysis for Triassic streams.

Sample	$-2 \ln \lambda$	*Degrees of freedom*	$\chi^2_{.05, DF}$	*Decision*
Mag 7	3.32	2	5.99	Accept

	Observed	*Sample size*	*Crit val*	*Decision*
Mag 8	16	24	17	Accept
Mag 9	9	16	12	Accept
Mag 10	10	16	10	Reject

Further examination indicates that the tributaries entering on the same side and flowing down-section are preferentially developed, in a ratio of about 2:1 over those flowing up-section. Thus it is concluded that an identifiable geological factor is influencing the topological arrangements in these small networks.

It is perhaps more remarkable that these drainage systems, which show strong geological control of their channel patterns, have no apparent systematic or identifiable bias in their topological properties above the level of the magnitude-4 networks cited above.

LINK PROBABILITIES

Introduction

The analysis has so far considered networks from magnitude 4 to magnitude 10 with varying degrees of topological resolution. To continue the statistical analysis to larger network sizes in a similar manner becomes increasingly difficult. For instance, the entire sample contains 25 magnitude-20 channel networks, while there exist 30 sets of possible stream numbers for that magnitude. Thus, it is necessary to devise a system which allows examination of topological properties of higher-magnitude systems.

In the preceding analysis, the TDCN has been considered the basic element and, as the network magnitude increased, TDCN's were grouped, by right-left classes, ambilateral classes and finally into stream-number sets. The strategy to be applied now is to examine a more fundamental element than the individual TDCN, namely the individual links. A coherent and consistent method of classifying links is developed. Then, a set of equations describing their frequency of occurrence for topologically random populations is derived, followed by examination of the sample networks in the context of these predictions.

The overall link-type classification and derivations which follow are largely abstracted from the published paper *A Classification of Channel Links in Stream Networks* (Mock 1971).

Link frequencies

In a topologically random population of channel networks of any given magnitude M, the probability of drawing a link at random of magnitude μ was given by eq 9, while the probability of drawing at random a link of magnitude μ from an infinite topologically random network was given by eq 10. It is possible to examine the frequency distribution of link magnitudes to test the hypothesis that the samples were drawn from an infinite topologically random population.

To properly test the hypothesis that a set of links could have been drawn from an infinite topologically random population requires that the links be randomly selected. The links which form the samples to be analyzed are the set of all links contained in a series of complete networks and do not represent random selection. The fact that they are complete networks puts certain limits on link magnitudes which would not be applicable had they been randomly selected. To illustrate this point consider the following differences between a random selection of 3117 links from an infinite topologically random population and the 3117 links that compose the contiguous-seven sample. The number of magnitude-1 links is rigorously set in the contiguous-seven sample while in a randomly selected sample it is not. There is no upper limit on the magnitude of a link in a randomly chosen sample while in the contiguous-seven sample it is 385 and is equal to the magnitude of the largest network in any sample consisting of integrated networks. The point is that selection of complete networks puts constraints on the possible outcomes and requires a certain restraint in interpretation of results. Table XIX shows the statistical data for the contiguous-seven and the Triassic samples.

Table XIX. Statistics and analysis of link-magnitude frequencies, contiguous-seven and Triassic streams.

Contiguous-seven Link magnitude	Observed	Expected	*Triassic* Link magnitude	Observed	Expected
2	420	389.6	2	214	210.3
3	214	193.3	3	104	105.8
4	123	121.8	4	47	65.7
5	74	85.2	5	44	46.0
6	54	63.9	6	34	34.5
7	34	50.2	7	29	27.1
8	31	40.8	8	24	22.0
9	23	34.0	9	15	18.4
10	22	28.9	10	16	15.6
> 10	558	548.0	> 10	314	295.7

Contiguous-seven: $-2ln\lambda = 21.58$, $\chi^2_{.05,9} = 16.92$
5% Decision: Reject

Triassic: $-2ln\lambda = 7.69$, $\chi^2_{.05,9} = 16.92$
5% Decision: Accept

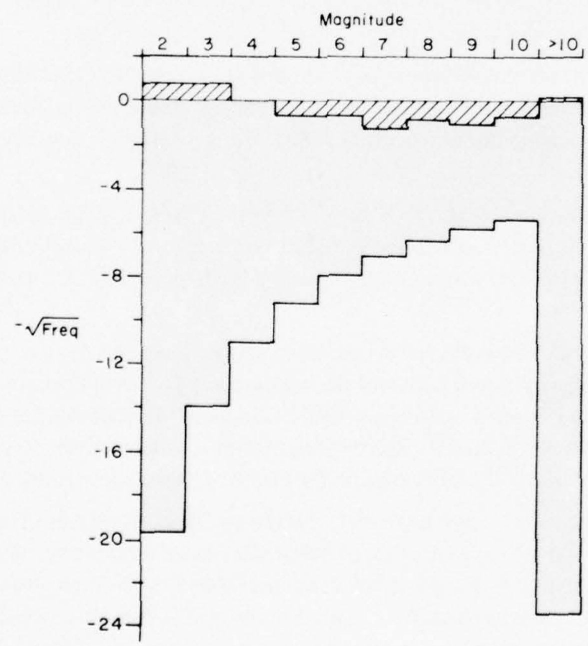

Figure 11. Hanging rootogram showing expected frequencies and deviations from expected frequencies as a function of magnitudes for the contiguous-seven networks.

The null hypothesis that the observed link frequencies could have been drawn from an infinite topologically random population can be rejected at the 0.05 confidence level for the contiguous-seven sample. In Figure 11, the contiguous-seven observed link frequencies and their deviations from predicted values are plotted by means of a hanging rootogram (James and Krumbein 1969). Figure 11 shows graphically the excess of observed magnitude-2 and -3 links and the dearth of observed links in the magnitude-5 -10 range, in comparison with the expected frequencies.

The observed deviations can be related to geological factors in the area of the contiguous-seven streams. The master channels, occupying strike valleys, are separated from each other by less easily eroded rock units. Networks tributary to the master channels are constrained by the intervening, more resistant rocks, to a size range governed in part by the spacing of the resistant rocks. Thus, depending upon local lithologies and structures, a certain range of link magnitudes will be depleted in frequency with respect to an infinite topologically random population.

Within the contiguous-seven streams the factors cited above appear to inhibit development of channel networks in the magnitude-5 to magnitude-10 range. The Triassic streams, on the other hand, do not show any similar trends.

Link types

Interior and exterior links have been defined in Chapter I. Within the set of interior links, James and Krumbein (1969) defined two further types: cis-links and trans-links. A cis-link was defined as an interior link bounded at its upper and lower forks by tributaries entering from the same side. A trans-link was defined as an interior link bounded at its forks by tributaries entering from opposite sides. A tributary, in the sense used here, is the link of lesser magnitude of the two links upstream from a junction. In the context of their study, James and Krumbein limited cis- and trans-links to those having a magnitude greater than 10. That restriction will be relaxed here, with no magnitude limits placed upon these link types.

In a topologically random population, cis- and trans-links occur with equal frequency. However, in the James and Krumbein study cited above, in a sample of 485 links, over 60% were trans-links, an occurrence with a probability of less than 0.00001 if the probability of occurrence of cis- and trans-links were equal.

A later study (Krumbein and Shreve 1970) in the same area (Inez quadrangle, Kentucky) but dealing with magnitude-5 networks, found trans-links occurring with greater frequency than cis-links, but not in sufficient quantity to justify rejecting the hypothesis that they have an equal probability of occurrence.

James and Krumbein (1969) proposed a model to explain observed cis- and trans-link length frequencies. At its headward end, a channel network grows by random bifurcations, but within the network channel adjustments take place, with coalescence of tributaries entering close to each other on the same side and thus extinction of some cis-links. While the model has been criticized (Abrahams 1972) it does satisfactorily explain the excess of trans-links in their study area.

The observed numbers of trans- and cis-links for the contiguous-seven and Triassic streams are shown in Tables XX and XXI as a function of magnitude. In an infinite topologically random population, the probability of occurrence of trans- and cis-links is the same, independent of their magnitude. The null hypothesis tested in Tables XX and XXI is that the cis- and trans-links could have been drawn from a population in which they occur with equal frequency. There is no reason to reject this hypothesis for either the contiguous-seven or Triassic samples when the total samples are considered. However when the link frequencies are examined as a function of magnitude, the null hypothesis can be rejected for three subsets, two in the contiguous-seven sample and one in the Triassic sample.

Table XX. Statistics and statistical analysis of trans- and cis-links for contiguous-seven streams.

Link magnitude	*Number of trans*	*% trans*	*Number of cis*	*Critical value*	*5% decision*
1-10	145	42.8	194	188	Reject
11-20	81	54.0	69	86	Accept
21-30	47	58.8	33	48	Accept
31-40	19	63.3	11	20	Accept
> 40	164	63.6	94	145	Reject
Total	456	53.2	401	458	Accept

Table XXI. Statistics and statistical analysis of trans- and cis-links for Triassic streams.

Link magnitude	*Number of trans*	*% trans*	*Number of cis*	*Critical value*	*5% decision*
1-10	98	47.3	109	118	Accept
11-20	21	36.2	37	36	Reject
21-30	21	47.7	23	28	Accept
31-40	12	57.1	9	15	Accept
> 40	88	54.0	75	94	Accept
Total	240	48.7	253	269	Accept

The earlier analysis of magnitude-4 TDCN from the contiguous-seven sample indicated a preferential development of what have now been designated cis-links. From Table XX it is clear that up to magnitude 10 there is a preferential development of the cis type. The same holds true for the Triassic sample although the frequency of occurrence of cis-links is not sufficiently different from that of trans-links for rejection of the null hypothesis. At the opposite end of the scale, i.e. for links with magnitudes greater than 40, exactly the opposite situation occurs. Both samples have more trans-links than cis-links, but the null hypothesis can be rejected only for the contiguous-seven sample.

The data shown in Tables XX and XXI and the analysis of magnitude-4 networks suggests the following hypothesis: in regions where trellis drainage patterns are developed bedrock attitude will preferentially favor certain flow directions. In low magnitude networks this will lead to more tributaries entering from the same side, hence more cis- than trans-links. At higher magnitudes, implying greater age, interaction of tributaries entering from the same side will eliminate some cis-links with an eventual predominance of trans-links.

Admittedly, the evidence which has suggested this hypothesis is hardly overwhelming and has certain ambiguities. For instance, the large percentage of low magnitude cis-links in the contiguous-seven sample as compared to the Triassic sample is consistent with its greater lithological diversity and bedrock dips, but the greater frequency of occurrence of trans-links at higher magnitudes is not. It is an area worth more study.

Exterior links. Two types of exterior links will be defined: 1) The S (source) link is a magnitude-1 link that joins another magnitude-1 link at its downstream fork. 2) The TS (tributary source) link is a magnitude-1 link that joins a link of magnitude greater than 1 at its downstream fork.

Magnitude of upstream link / Magnitude of downstream link	$= \frac{1}{2}\mu$ $Q(\mu; M)$	$\neq \frac{1}{2}\mu$ $K(\mu; M)$
$< 2\mu$ $S(\mu; M)$	B-link $P(\mu_B; M)$	CT-link $P(\mu_{CT}; M)$
$\geq 2\mu$ $T(\mu; M)$	TB-link $P(\mu_{TB}; M)$	T-link $P(\mu_T; M)$

Figure 12. Definition of link types by the magnitude relationships of link of magnitude μ and its adjacent upstream and downstream neighbors.

Interior links. Figure 12 shows the upstream and downstream criteria for defining interior links. 1) The B (bifurcating) link is a link of magnitude μ that is formed at its upstream fork by the confluence of two links, each of magnitude $\mu/2$, and that flows at its downstream fork into a link of magnitude less than 2μ. 2) A TB (tributary bifurcating) link is a link of magnitude μ that is formed at its upstream fork by the confluence of two links, each of magnitude $\mu/2$, and that flows at its downstream fork into a link of magnitude greater than or equal to 2μ. 3) The T (tributary) link is a link of magnitude μ that is formed at its upstream fork by the confluence of two links of unequal magnitude and that flows at its downstream fork into a link of magnitude greater than or equal to 2μ. 4) The CT-(cis-trans) link is a link of magnitude μ that is formed at its upstream fork by the confluence of two links of unequal magnitude and that flows at its downstream fork into a link of magnitude less than 2μ. Figure 13 shows an idealized network illustrating the link types.

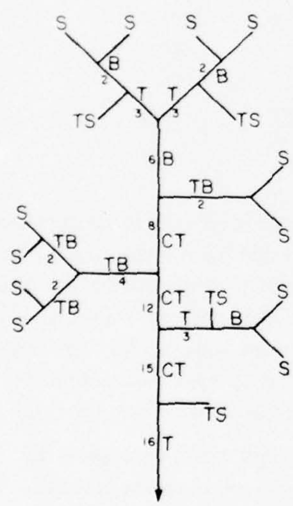

Figure 13. Idealized network showing link magnitudes and types.

The last downstream link in any system under study, i.e. the highest magnitude link, is defined as either a T- or TB-link depending on the magnitude relationships at its upstream fork.

Note that the CT category of links includes the cis- and trans-links defined by James and Krumbein (1969). Cis- and trans-links are not considered individually since they are dependent on topologic relationships as well as magnitude relationships at successive forks, while the criteria used here are based entirely on arithmetic relationships of the link magnitudes.

Since link types have been defined in terms of magnitude relationships, eq 9 and 10 provide the bases for calculation of the probability of occurrence of each link type in finite and infinite topologically random networks.

Probability of occurrence

Exterior links. Exterior links are by definition links of magnitude 1. The probability of drawing an exterior link at random from a topologically random population of networks of magnitude M is given by eq 9, with $\mu = 1$. Designating this as $P(\text{ext}; M)$ it is

$$P(\text{ext}; M) = \omega(1; M) = M/(2M-1). \tag{12}$$

The probability of drawing an exterior link at random from an infinite topologically random population is

$$P(\text{ext}) = \lim_{M\to\infty} M/(2M-1) = 0.5.$$

Draw a link at random from a topologically random population of networks of magnitude M. If the link is of magnitude 1, what is the probability that it connects with another magnitude-1 link? The original draw leaves a topologically random population of magnitude $M-1$. The original link has an equal probability of connecting with any one of the $2M-3$ remaining links. The probability that it connects with another magnitude-1 link is equal to the proportion in which the magnitude-1 links occur or $(M-1)/(2M-3)$. Thus, the probability of occurrence of an S-link is

$$P(S; M) = \frac{M}{2M-1} \times \frac{M-1}{2M-3} \tag{13}$$

and the probability of occurrence of S-links in an infinite topologically random population is

$$P(S) = \lim_{M\to\infty} \frac{M(M-1)}{(2M-1)(2M-3)} = 0.25. \tag{14}$$

To determine the probability of drawing a TS-link, a similar type of argument is used.

A link is drawn at random. If it is a magnitude-1 link, determine the probability that it connects with an interior link in the $(M-1)$-magnitude network which remains. The probability of drawing at random an interior link from a topologically random population of magnitude-M networks is (using eq 12):

$$P(\text{int}; M) = 1-P(\text{ext}; M) = (M-1)/(2M-1). \tag{15}$$

The probability of occurrence of TS-links is given by

$$P(TS; M) = \frac{M}{2M-1} \times P(\text{int}; M-1)$$

$$P(TS; M) = \frac{M}{2M-1} \times \frac{M-2}{2M-3}\,, \tag{16}$$

for topologically random populations of magnitude M and by

$$P(TS) = \lim_{M\to\infty} \frac{M}{2M-1} \times \frac{M-2}{2M-3} = 0.25, \tag{17}$$

for an infinite topologically random network.

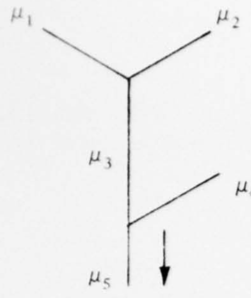

Figure 14. The randomly drawn link μ_3, and the four links to which it is attached. The arrow designates the flow direction.

Interior links. The essence of the rather heuristic arguments to be presented is that a series of successive random selections of links from topologically random populations of appropriately sized networks will serve to define interior link types. Consider a topologically random population of networks of magnitude M. From this population a link of magnitude μ, designated as μ_3, is randomly drawn. Along with the link μ_3, the four links joined to μ_3 at its upper and lower junctions are shown in Figure 14.

From the definition of link magnitudes it is known only that

$$\mu_1 + \mu_2 = \mu_3$$

$$\mu_3 + \mu_4 = \mu_5 .$$

In terms of the defining criteria shown in Figure 12 the possible types of μ_3 are:

μ_3 = B-link if μ_1 or $\mu_2 = \mu_3/2$ and $\mu_5 < 2\mu$
μ_3 = TB-link if μ_1 or $\mu_2 = \mu_3/2$ and $\mu_5 \geq 2\mu$
μ_3 = CT-link if μ_1 or $\mu_2 \neq \mu_3/2$ and $\mu_5 < 2\mu$
μ_3 = T-link if μ_1 or $\mu_2 \neq \mu_2/2$ and $\mu_5 \geq 2\mu$.

In the following discussion reference to a network of any stated magnitude will refer to a topologically random population of such networks, and random selection of a link will mean random selection from a topologically random population of the specified magnitude.

Consider now the link μ_3. It is the ultimate link of a sub-network of magnitude μ_3, imbedded in the overall network of magnitude M. Since the link was randomly selected from a topologically random population the possible topological arrangements of its network form a topologically random population of magnitude μ_3. Since $\mu_1 + \mu_2 = \mu_3$ only the magnitude of one of the two upstream links is independent and need be considered. Taking μ_1, it can have any magnitude from 1 to $(\mu_3 - 1)$ and the sub-network which it defines is a topologically random population of networks of magnitude $(\mu_3 - 1)$. Thus the probability that $\mu_1 = \mu_3/2$, denoted as $q(\mu_3; M)$ is, using eq 11,

$$q(\mu_3; M) = \omega(\mu_3/2; \mu_3 - 1).$$

In the general case then, the probability that a randomly selected link from a topologically random population of networks of magnitude M will bifurcate at its upper junction is

$$q(\mu; M) = \omega(\mu/2; \mu - 1)$$

and the probability of occurrence is

$$Q(\mu; M) = \omega(\mu; M)\, \omega(\mu/2; \mu - 1). \tag{18}$$

Since there is only one other possibility, the probability that the link μ does not bifurcate at its upper junction is

$$k(\mu; M) = 1 - \omega(\mu/2; \mu - 1)$$

and

$$K(\mu; M) = \omega(\mu; M)\,[1 - \omega(\mu/2; \mu-1)]\ . \tag{19}$$

Note that $q(\mu; M)$ and $k(\mu; M)$ are independent of M. Such is not the case for the downstream possibilities relating μ_3, μ_4 and μ_5.

The two possibilities at the downstream junction of link μ_3, shown in Figure 14, are

$$\mu_5 < 2\mu_3 \Rightarrow \mu_4 < \mu_3,$$

and

$$\mu_5 \geq 2\mu_3 \Rightarrow \mu_4 \geq \mu_3\ .$$

It is convenient to work with μ_4 rather than μ_5, so that the probabilities of interest are, having randomly selected μ_3, the probability that it joins a link $\mu_4 < \mu_3$ or that it joins a link $\mu_4 \geq \mu_3$. Remembering that these are topologically random populations, the effect of selecting μ_3 is to remove all links tributary to it from the population of magnitude-M networks. That is, the remaining population is now a topologically random population of diminished magnitude $(M - \mu_3)$. Since μ_3 can join any link in the diminished network, the problem is reduced to the problem of randomly selecting a link of magnitude μ_4 from the networks of $(M-\mu_3)$ magnitude. Thus, the probability that $\mu_4 < \mu_3$ is

$$s(\mu_3; M) = \sum_{\mu_4=1}^{\mu_3-1} \omega(\mu_4; M-\mu_3)$$

and for the general case, designating the second link as γ, the equation is

$$s(\mu; M) = \sum_{\gamma=1}^{\mu-1} \omega(\gamma; M-\mu)$$

and summing over all possibilities the probability of occurrence is

$$s(\mu; M) = \sum_{\mu=1}^{M} \sum_{\gamma=1}^{\mu-1} \omega(\mu; M)\,\omega(\gamma; M-\mu). \tag{20}$$

The probability that $\gamma \geq \mu$ is then given by

$$t(\mu; M) = 1 - \sum_{\gamma=1}^{\mu-1} \omega(\gamma; M-\mu)$$

and

$$T(\mu; M) = \sum_{\mu=1}^{M} \omega(\mu; M) \left[1 - \sum_{\gamma=1}^{\mu-1} \omega(\gamma; M-\mu)\right]. \tag{21}$$

Equations 18-21 define the probability of occurrence of the defining criteria for topologically random populations of magnitude-M networks.

The probability of drawing a link of specified μ which satisfies a set of upstream and downstream relationships is simply the intersection of the three probability spaces $\omega(\mu; M)$, $q(\mu; M)$ or $k(\mu; M)$, and $s(\mu; M)$ or $t(\mu; M)$. Designating this as $P(\mu_{\text{type}}; M)$ as shown in Figure 12 the probabilities are:

$$P(\mu_{\text{B}}; M) = \omega(\mu; M)\, q(\mu; M)\, s(\mu; M)$$
$$P(\mu_{\text{TB}}; M) = \omega(\mu; M)\, q(\mu; M)\, t(\mu; M)$$
$$P(\mu_{\text{CT}}; M) = \omega(\mu; M)\, k(\mu; M)\, s(\mu; M)$$
$$P(\mu_{\text{T}}; M) = \omega(\mu; M)\, k(\mu; M)\, t(\mu; M).$$

Finally, to define the probability of occurrence of a particular type of link in a topologically random population of magnitude-M networks it is necessary to sum over all possibilities. Designating this as $P(\text{type}; M)$ the equations are:

$$P(B; M) = \sum_{\mu=1}^{M} P(\mu_{\text{B}}; M) = \sum_{\mu=1}^{M} \sum_{\gamma=1}^{\mu-1} \omega(\mu; M)\, \omega(\mu/2; \mu-1)\, \omega(\gamma; M-\mu) \tag{22}$$

$$P(TB; M) = \sum_{\mu=1}^{M} P(\mu_{\text{B}}; M) = \sum_{\mu=1}^{M} \omega(\mu; M)\, \omega(\mu/2; \mu-1) \left[1 - \sum_{\gamma=1}^{\mu-1} \omega(\gamma; M-\mu)\right], \tag{23}$$

$$P(CT; M) = \sum_{\mu=1}^{M} P(\mu_{\text{CT}}; M) = \sum_{\mu=1}^{M} \sum_{\gamma=1}^{\mu-1} \omega(\mu; M)\, [1 - \omega(\mu/2; \mu-1)]\, \omega(\gamma; M-\mu) \tag{24}$$

and

$$P(T; M) = \sum_{\mu=1}^{M} P(\mu_{\text{T}}; M) =$$

$$\sum_{\mu=1}^{M} \left\{ \omega(\mu; M) \left[1 - \omega(\mu/2; \mu-1)\right] \left[1 - \sum_{\gamma=1}^{\mu-1} \omega(\gamma; M-\mu)\right] \right\} - \omega(1; M). \tag{25}$$

The quantity $\omega(1; M)$ in eq 25 removes the exterior links which are included in the summation.

It is of interest to determine the limiting values, if any, of the probabilities expressed in eq 22-25 as M becomes infinite, i.e. for an infinite topologically random network. The approach is to calculate analytically the marginal probabilities shown in Figure 12 for the infinite case and then to evaluate numerically the joint probabilities $P(B; M)$ and $P(TB; M)$, which are sufficient to define the remaining joint probabilities. It can be shown that

$$\sum_{\mu=1}^{M} \omega(\mu; M)\, \omega(\mu/2; \mu-1) = \frac{1}{2} \sum_{\mu=1}^{M} \omega(\mu/2; M)\, \omega[\mu/2; M - (\mu/2)] =$$

$$\frac{1}{2} \sum_{\mu=1}^{M} \omega(\mu; M)\, \omega(\mu; M-\mu).$$

Thus, the marginal probability $Q(\mu; M)$ of Figure 12 can be rewritten as

$$Q(\mu; M) = \frac{1}{2} \sum_{\mu=1}^{M} \omega(\mu; M)\, \omega(\mu; M - \mu). \tag{26}$$

Shreve (1967, p. 181) has shown that

$$\lim_{M\to\infty} \omega(\mu; M) = \frac{2^{-(2\mu-1)}}{2\mu-1} \binom{2\mu-1}{\mu} = \nu(\mu),$$

so that eq 26 can be rewritten as

$$\lim_{M\to\infty} Q(\mu; M) = \frac{1}{2} \sum_{\mu=1}^{\infty} \nu(\mu)\nu(\mu). \tag{27}$$

This summation can be calculated exactly by using the functional relationships satisfied by the gamma function (M. Dacey, personal communication, 1970), which gives

$$\lim_{M\to\infty} Q(\mu; M) = \frac{1}{2} [(4/\pi) - 1] = 0.13622\ldots . \tag{28}$$

Thus,

$$\lim_{M\to\infty} K(\mu; M) = 1 - 0.13662 - 0.5 = 0.36338\ldots . \tag{29}$$

The remaining marginal probabilities for the infinite topologically random case become

$$\lim_{M\to\infty} S(\mu; M) = \sum_{\mu=1}^{\infty} \sum_{\gamma=1}^{\mu-1} \nu(\mu)\, \nu(\gamma) \tag{30}$$

and

$$\lim_{M\to\infty} T(\mu; M) = \sum_{\mu=1}^{\infty} \sum_{\gamma=\mu}^{\infty} \nu(\mu)\, \nu(\gamma). \tag{31}$$

Consider now an infinite topologically random network from which two consecutive random drawings are made designating the magnitude of the first link μ and the second link γ. Designate the joint probabilities of $\nu(\mu)\, \nu(\gamma)$ as $\nu(\mu, \gamma)$; then a matrix of probabilities, as shown in Figure 15, is symmetric. Because of symmetry,

$$\sum_{\mu=2}^{\infty} \sum_{\gamma=1}^{\mu-1} \nu(\mu, \gamma) = \sum_{\mu=1}^{\infty} \sum_{\gamma=\mu+1}^{\infty} \nu(\mu, \gamma) \tag{32}$$

$$
\begin{array}{c|ccccc}
 & \multicolumn{5}{c}{\nu(\gamma)\rightarrow} \\
 & 1 & 2 & 3 & \ldots & \infty \\
\hline
1 & \nu(1,1) & \nu(1,2) & \nu(1,3) & \ldots & \nu(1,\infty) \\
2 & (2,1) & (2,2) & & & \\
3 & \nu(3,1) & & & & \\
 & \cdot & & & & \\
\nu(\mu)\downarrow & \cdot & & & & \\
 & \cdot & & & & \\
\infty & \nu(\infty,1) & & & &
\end{array}
$$

Figure 15. Probability matrix for an infinite topologically random network.

$$\sum_{\mu=2}^{\infty}\sum_{\gamma=1}^{\mu-1} \nu(\mu, \gamma) + \sum_{\mu=1}^{\infty}\sum_{\gamma=1}^{\infty} \nu(\mu, \gamma) + \sum_{\mu=1}^{\infty} \nu(\mu, \mu) = 1 \tag{33}$$

but

$$\sum_{\mu=2}^{\infty}\sum_{\gamma=1}^{\mu-1} \nu(\mu, \gamma) = \sum_{\mu=1}^{\infty}\sum_{\gamma=1}^{\mu-1} \nu(\mu, \gamma) = \lim_{M\to\infty} S(\mu; M).$$

Since, for $\mu = 1$,

$$\sum_{\gamma=1}^{\mu-1} \nu(\mu, \gamma) = 0$$

from eq 32 and 33,

$$2 \lim_{M\to\infty} S(\mu; M) = 1 - \sum_{\mu=1}^{\infty} \nu(\mu; \mu), \tag{34}$$

$$\lim_{M\to\infty} S(\mu; M) = 0.36338,$$

and

$$\lim_{M\to\infty} T(\mu; M) = 0.63662. \tag{35}$$

Now the limits of $P(B; M)$ and $P(TB; M)$ as $M\to\infty$ can be evaluated;

$$\lim P(B; M) + \lim P(TB; M) = \lim Q(\mu; M) = 0.13662,$$

which is

$$\sum_{\mu=1}^{\infty}\sum_{\gamma=1}^{\mu-1} \nu(\mu)\,\omega(\mu/2;\mu-1)\,\nu(\gamma) = \sum_{\mu=1}^{\infty}\sum_{\gamma=\mu}^{\infty} \nu(\mu)\,\omega(\mu/2;\mu-1)\,\nu(\gamma) = 0.13662. \tag{36}$$

Equation 36 can be rapidly evaluated to five significant figures by means of a computer, so that

$$\lim_{M\to\infty} P(B;M) = 0.07086, \tag{37}$$

$$\lim_{M\to\infty} P(TB;M) = 0.06576, \tag{38}$$

and using the remaining marginal probabilities of Figure 12

$$\lim_{M\to\infty} P(CT;M) = 0.29252 \tag{39}$$

and

$$\lim_{M\to\infty} P(T;M) = 0.07086. \tag{40}$$

Table XXII shows the probability of occurrence of each link type for topologically random populations of various magnitudes.

In Table XXII note that the probability of occurrence of T- and B-links is the same. It is implicit in the defining criteria that, on moving upstream from a T-link, a main channel sequence must terminate at a B-link. This holds true for any channel sequence within a network, thus giving a one for one correspondence of T-links and B-links. Thus, although six types of links have been defined, two exterior and four interior, there are only three independent link categories.

Table XXII. Probability of occurrence of link types for networks of various magnitudes.

M	$P(S;M)$	$P(TS;M)$	$P(CT;M)$	$P(T;M)$	$P(B;M)$	$P(TB;M)$
2	0.667					0.333
3	0.400	0.200		0.200	0.200	
4	0.343	0.229	0.114	0.114	0.114	0.086
5	0.317	0.238	0.159	0.111	0.111	0.063
6	0.303	0.242	0.182	0.100	0.100	0.074
7	0.294	0.245	0.200	0.098	0.098	0.065
8	0.287	0.246	0.213	0.091	0.091	0.071
9	0.282	0.247	0.224	0.090	0.090	0.067
10	0.279	0.248	0.231	0.087	0.087	0.069
20	0.263	0.249	0.264	0.078	0.078	0.067
50	0.255	0.250	0.281	0.074	0.074	0.066
100	0.253	0.250	0.287	0.072	0.072	0.066
200	0.251	0.250	0.290	0.072	0.072	0.066
400	0.251	0.250	0.291	0.071	0.071	0.066
∞	0.250	0.250	0.293	0.071	0.071	0.066

Tables XXIII–XXVI give the statistics and statistical analyses for link types of the contiguous-seven and Triassic streams. There is no reason to reject the hypothesis that the Triassic sample was drawn from an infinite topologically random population. However the hypothesis can be rejected for the case of the contiguous-seven networks. As shown in Table XXV, we can also reject the hypothesis that the interior and exterior types occur with the frequencies expected in a topologically random population.

Table XXIII. Link-type statistics for the contiguous-seven streams.

Link type	*Observed*	*Expected*
CT	856	913.3
T	238	221.3
B	238	221.3
TB	223	205.7
S	844	779.3
TS	718	779.3

Table XXIV. Link-type statistics for Triassic streams.

Link type	*Observed*	*Expected*
CT	493	493.7
T	119	119.6
B	119	119.6
TB	110	111.2
S	432	421.3
TS	412	421.3

Table XXV. Statistical analysis of link types for contiguous-seven streams.

Sample	*Degrees of freedom*	*-2lnλ*	*Crit val*	*5% decision*
All link types	3	18.13		Reject
Interior link types	2	7.61		Reject
S- vs TS-links			820	Reject

Table XXVI. Statistical analysis of link types for Triassic streams.

Sample	*Degrees of freedom*	*-2lnλ*	*Crit val*	*5% decision*
All link types	3	0.58		Accept
Interior link types	2	0.006		Accept
S- vs TS-links			451	Accept

The deviations observed from predicted link type in the contiguous-seven sample are consistent with the link-magnitude deviations shown in Table XIX and Figure 9. A large part of the deviation of CT-links is a result of the less-than-expected number of magnitude-5 through magnitude-10 links, and at least part of the excess in TB- and T-links corresponds to the greater-than-expected number of magnitude-2 links.

Joint probability for link magnitude and type

It is now possible to construct the joint-probability distribution for link type and link magnitude for an infinite topologically random population using eq 22–25. The resulting probabilities are shown in Table XXVII.

Table XXVII. Joint probabilities of interior-link types and magnitude for an infinite topologically random channel network.

μ	*Trans*	*Cis*	*T*	*B*	*TB*	$\nu(\mu)$
2	0	0	0	.06250	.0625	.12500
3	.01953	.01953	.02344			.06250
4	.01074	.01074	.00977	.00537	.00244	.03906
5	.00993	.00993	.00748			.02734
6	.00699	.00699	.00457	.00147	.00048	.02051
7	.00624	.00624	.00363			.01611
8	.00487	.00487	.00258	.00060	.00016	.01309
9	.00438	.00438	.00214			.01091
10	.00362	.00362	.00165	.00030	.00007	.00927
> 10	.07996	.07996	.01560	.00062	.00001	.17621
P(type)	.14626	.14626	.07086	.07086	.06566	.50000

Tables XXVIII and XXIX show the observed and predicted numbers of links as a function of link type and link magnitude. The predicted values are those expected for random selection of samples of equivalent sizes from an infinite topologically random population. As was discussed previously, the samples do not consist of randomly selected links, thus a certain bias will occur. This implies that rejection of the null hypothesis that the observed frequencies could have been drawn from an infinite topologically random population will have some ambiguity. For convenience the statistic $U = (\text{Observed–Expected})^2/\text{Expected}$ has been calculated. This statistic follows the chi-square distribution so that if $U > \chi^2_{\alpha,\mathrm{DF}}$ the null hypothesis can be rejected at the α confidence level.

The results of the statistical analyses are included in Tables XXVIII and XXIX. There is no reason to reject the null hypothesis in the case of the Triassic sample. For the contiguous-seven sample the null hypothesis can be rejected for each of the following:

a. The total sample.
b. The total sample with cis- and trans-links combined.
c. The subset consisting of all links up to and including magnitude 10.
d. The subset defined in c. but with cis- and trans-links combined.

The results are consistent with many of the earlier results, and enable specific identification of where deviations from expectation occur. For example, in Table XIX magnitude-3 links were observed to occur with greater frequency than predicted. Table XXVIII shows that the major part of the deviation is accounted for by the large number of T-links. In fact T-links occur with greater than expected frequency up to and including magnitude 5, as do also TB-links. This means that there are more small, but complete, networks in the sample than would be expected in a topologically random population.

Table XXVIII. Observed and expected (in parentheses) frequencies of interior links as a function of link type and link magnitude. Expected frequencies are those expected from a random selection from an infinite topologically random population. Contiguous-seven sample.

Link magnitude	*Link types*				
	Trans	*Cis*	*T*	*B*	*TB*
2				214 (202.2)	208 (187.4)
3	51 (60.9)	65 (60.9)	98 (73.0)		
4	28 (33.5)	34 (33.5)	34 (30.5)	17 (16.7)	10 (7.6)
5	15 (31.0)	25 (31.0)	34 (23.3)		
6	18 (21.8)	16 (21.8)	14 (14.2)	1 (4.6)*	5 (1.5)*
7	10 (19.5)	18 (19.5)	6 (11.3)	*	*
8	5 (15.2)	16 (15.2)	6 (8.0)	4 (1.9)*	0 (0.2)*
9	8 (13.7)	13 (13.7)	2 (6.7)*	*	*
10	10 (11.3)	7 (11.3)	3 (5.1)*	2 (0.9)*	0 (0.2)*
> 10	310 (249.2)	207 (249.2)	41 (48.6)	0 (1.9)*	0 0*

* Combined for statistical analysis

Sample	*DF*	*U*	$\chi^2_{.05,\,DF}$	*5% decision*
Total	18	83.5	28.87	Reject
$\mu > 10$ excluded	18	60.3	28.87	Reject
Total with cis and trans combined	10	49.9	18.31	Reject
Cis-trans combined, $\mu > 10$ excluded	10	48.0	18.31	Reject

Table XXIX. Observed and expected (in parentheses) frequencies of interior links as a function of link type and link magnitude. Expected frequencies are those expected from random selection from an infinite topologically random population. Triassic sample.

Link magnitude	*Link types*				
	Trans	*Cis*	*T*	*B*	*TB*
2				105 (109.3)	108 (101.3)
3	25 (32.9)	28 (32.9)	52 (39.5)		
4	11 (18.1)	17 (18.1)	10 (16.5)	8 (9.0)	1 (4.1)
5	16 (16.7)	18 (16.7)	10 (12.6)		
6	12 (11.8)	13 (11.8)	5 (7.7)	4 (2.5)	0 (0.8)
7	14 (10.5)	9 (10.5)	6 (6.1)		
8	10 (8.2)	8 (8.2)	5 (4.3)	0 (1.0)	1 (0.3)
9	4 (7.4)	8 (7.4)	3 (3.6)		
10	6 (6.1)	8 (6.1)	1 (2.8)	1 (0.5)	0 (0.1)
> 10	142 (134.7)	144 (134.7)	27 (26.3)	1 (1.0)	0 0

* Combined for statistical analysis

Sample	*DF*	*U*	$\chi^2_{.05,\,DF}$	*5% decision*
Total	11	18.66	19.68	Accept

Abrahams (1972) has cited the significance of "maximum extension" in the study of the frequency distribution of interior-link lengths. Paraphrasing Glock (1931), as quoted by Abrahams (1972, p. 731), maximum extension is the time when a drainage system is fully developed. In a trellis pattern drainage network the master channels extend headward, usually along-strike; when a bifurcation occurs, that link which is growing across-strike has a much more limited potential for growth than its sister link. This arises from the fact that another master channel exists, at some distance depending upon local geology, developing parallel to the first channel. Thus, cross-strike channels are constrained to reach their maximum development within an area bounded by the master streams. The net result one would expect is what has been observed in the contiguous-seven sample, an excess of low-magnitude tributaries over what should be expected in a randomly bifurcating system.

LINK LENGTHS

Introduction

In previous chapters a systematic study of a sample of real channel networks has been made, comparing observed properties with those predictable from a topologically random model. A classification of channel-link types was devised to enable the study to proceed at a level different from that of past work. The question arises: Do the link types defined on pages 28-30 differ from each other in any way other than in the numerical relationships of links at their upper and lower forks? Are there physical or geometric differences between link types, or are they only definable in the context of a particular numeration scheme?

The above question is the subject of this section. In examining this question, the idea of topological randomness or nonrandomness can be left aside as not germane, at least at the level of simply determining if a physical difference exists between link types. Furthermore, the fact that the sample under study here has been drawn from a particular type of stream pattern largely controlled by geology will be disregarded in the analysis, although it may be a caveat in the conclusions.

Link lengths

The particular property of links to be examined here is their length. Two reasons exist for this, one that it is the simplest property, other than magnitude, to measure from a map of a channel network and two, there is a limited amount of pre-existing work on link lengths.

Previous work

Strahler (1954) and Schumm (1956) showed that length-frequency distributions of 1st-order streams, i.e. exterior links, could be well represented by a log normal distribution. Smart (1968, p. 1005) made the following assumption: lengths of interior links in a given network are independent random variables drawn from the same population. Later in the same paper, he introduced a negative exponential density as a specific model for the interior-link-length-frequency distribution. Shreve (1969) proposed a gamma density with a shape factor of 2 as a model for interior-link lengths. These models have had varying degrees of success in describing observed interior-link-length distributions. The most detailed study was conducted by James and Krumbein (1969) in which they developed models for the distribution of trans-links and cis-links.

Observed link-length frequency distribution

Observed interior-link-length frequency distributions for the contiguous-seven and Triassic networks are shown in Figure 16. The basic assumption at the start will be that cited above, namely that the lengths of interior links in a given network are independent random variables drawn from the same population. The following hypothesis will be tested: The link-length-frequency distributions for each interior-link type were drawn from the same population as the total interior-link-length-frequency distribution. Note that no specific population models are implied here.

Statistical analysis of interior links

The null hypothesis to be tested is: link-length frequencies are independent of link type. Tables XXX and XXXI show the observed and expected link-length frequencies calculated under the assumption that they were all drawn from the same population. These tables are contingency tables for a two-way classification. The null hypothesis can be rejected at the 0.05 confidence level for both samples.

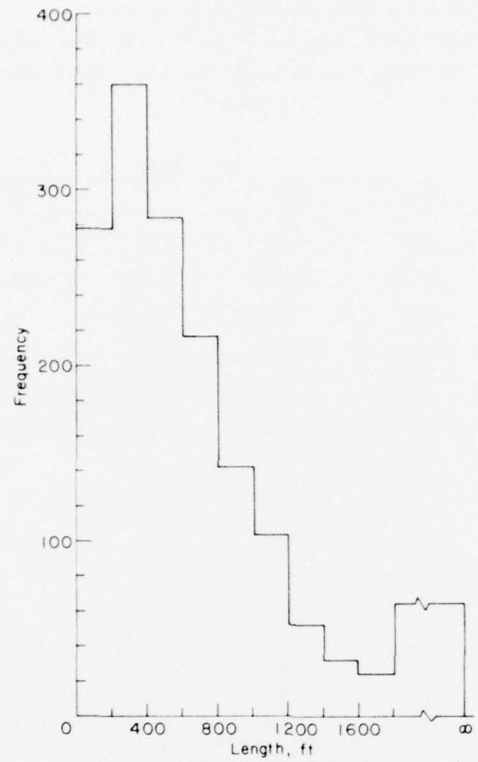

a. Contiguous-seven networks.

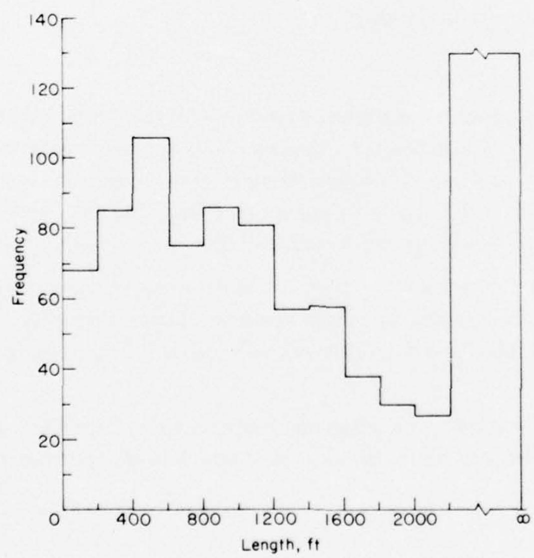

b. Triassic networks.

Figure 16. Observed interior-link-length frequency distributions.

Table XXX. Contingency table showing length frequencies versus link type for the contiguous-seven sample. Numbers in parentheses are expected frequencies calculated under the assumption that link type and length frequency are independent.

Length	*Type*				
(ft)	*Trans*	*Cis*	*T*	*B*	*TB*
0-200	138	43	14	54	29
	(81.3)	(71.7)	(42.5)	(42.5)	(39.9)
200-400	100	98	39	71	52
	(105.3)	(92.8)	(55.1)	(55.1)	(51.6)
400-600	69	94	47	36	38
	(82.1)	(73.2)	(43.5)	(43.5)	(40.7)
600-800	58	53	40	34	31
	(53.2)	(55.7)	(33.1)	(33.1)	(31.0)
800-1000	34	41	23	20	24
	(41.5)	(36.6)	(21.7)	(21.7)	(20.4)
1000-1200	21	23	32	10	17
	(30.1)	(26.6)	(15.8)	(15.8)	(14.8)
1200-1400	10	16	14	5	7
	(15.2)	(13.4)	(8.0)	(8.0)	(7.5)
> 1400	25	33	29	8	25
	(35.1)	(30.9)	(18.4)	(18.4)	(17.2)

$\chi^2 = 149.83$

$\chi^2_{.05,\,21} = 32.67$; Decision: Reject

While these tests allow rejection of the null hypothesis for the total samples, they do not provide much insight into any similarities between pairs of link types. To examine this further a series of contingency tests was made for each sample, comparing the length-frequency distribution of each link type successively with those of the other link types. The null hypothesis is that the length-frequencies of each type in the pair could have been drawn from the same population.

The results, shown in Tables XXXII and XXXIII, support the view that several link-length populations are present. In addition the length-frequency distributions of S- and TS-links are compared and tested in the tables, and the null hypothesis rejected for the contiguous-seven and Triassic samples.

Another approach is to consider the mean link length of each of the five interior-link types. The samples are sufficiently large to justify large-sample methods, and use of the statistic

$$\omega = \frac{\bar{X}_1 - \bar{X}_2}{\left(\frac{S_1^2}{n_1} + \frac{S_2^2}{n_2}\right)^{1/2}}$$

Table XXXI. Contingency table showing length frequencies versus link type for the Triassic sample. Numbers in parentheses are expected frequencies calculated under the assumption that link type and length frequency are independent.

Length (ft)	Type: Trans	Cis	T	B	TB
0-200	29 (19.4)	14 (20.5)	6 (9.6)	11 (9.6)	8 (8.9)
200-400	37 (24.3)	18 (25.6)	7 (12.0)	15 (12.0)	8 (11.1)
400-600	37 (30.2)	30 (31.9)	14 (15.0)	13 (15.0)	12 (13.9)
600-800	15 (21.4)	28 (22.6)	8 (10.6)	15 (10.6)	9 (9.8)
800-1000	20 (24.5)	35 (25.9)	10 (12.2)	10 (12.2)	11 (11.2)
1000-1200	28 (23.1)	18 (24.4)	9 (11.5)	14 (11.5)	12 (10.6)
1200-1400	10 (16.3)	22 (17.1)	7 (8.1)	11 (8.1)	7 (7.5)
> 1400	64 (80.8)	88 (85.1)	58 (40.0)	30 (40.0)	43 (37.0)

$\chi^2 = 57.98$

$\chi^2_{.05,\,21} = 32.67$; Decision: Reject

Table XXXII. Results of two-way contingency tests of link type pairs and length frequencies for the contiguous-seven sample. Column labeled $P(\omega)$ is explained in text.

	χ^2	DF	Decision	$P(\omega)$
Trans-Cis	52.15	7	Reject	.001
Trans-T	72.00	7	Reject	.001
Trans-B	8.89	7	Accept	.9
Trans-TB	24.36	7	Reject	.001
Cis-T	22.81	7	Reject	.001
Cis-B	24.78	7	Reject	.01
Cis-TB	6.57	7	Accept	.35
T-B	52.70	7	Reject	.001
T-TB	16.19	7	Reject	.019
B-TB	14.37	7	Reject	.003
S-TS	115.11	8	Reject	.001

$\chi^2_{.05,\,7} = 14.07$

Table XXXIII. Results of two-way contingency test of link type pairs and length frequencies for the Triassic sample. Column labeled $P(\omega)$ is explained in text.

	χ^2	*DF*	*Decision*	*P(ω)*
Trans-Cis	30.79	8	Reject	.007
Trans-T	24.28	8	Reject	.001
Trans-B	9.86	8	Accept	.9
Trans-TB	16.53	8	Reject	.01
Cis-T	8.73	8	Accept	.17
Cis-B	11.09	8	Accept	.008
Cis-TB	7.84	8	Accept	.29
T-B	17.44	8	Reject	.001
T-TB	5.27	8	Accept	.96
B-TB	8.87	8	Accept	.009
S-TS	50.16	8	Reject	.002

$\chi^2_{.05,\,8} = 15.51$

where X_i is the mean link length, S_i^2 is the sample variance, and n_i is the sample size. For large sample sizes, ω asymptotically approaches zero mean and unit standard deviation (Rao 1952, p. 217). ω is then a measure, in Gaussian standard deviation units, of the difference between the means; thus, the probability that the two sample means were drawn from populations having the same mean can be taken from normal probability tables. The ω statistic was calculated for each link pair and, if 0.05 probability is used as a decision criterion, similar results to those obtained with the contingency tests will be obtained with the following exceptions: the cis-B and B-TB link pairs from the Triassic sample can be rejected. The columns labeled $P(\omega)$ in Tables XXXII and XXXIII are the probabilities that the sample means were drawn from populations having the same mean link length.

The results of these tests imply that there exists a relationship between link type and length frequency distributions, i.e. there are different populations for certain of the link types. This is summarized in Table XXXIV where the link pairs which appear to be drawn from different populations are tabulated.

As a final but qualitative demonstration of the relationship between link type and link length, consider the data shown in Table XXXV, where link types for the two samples are listed in descending order of mean link length. If link types and length are related, then a similar sequence of types as a function of length should occur. As can be seen in Table XXXV, there is a similarity in the sequences. This is illustrated graphically in Figure 17 where the mean lengths of link types from the contiguous-seven networks are plotted versus the corresponding mean link length from the Triassic networks. The solid line is a least-squares regression line having a correlation coefficient of 0.898, significant at the 0.01 level. No predictive capability is implied by Figure 17; rather it indicates that the link type and link length properties behave similarly in two widely separated samples.

Summary

The link types developed in the section *Link Probabilities* (p. 26) have been examined in the context of their length-frequency distributions. Statistical tests strongly imply that the lengths of interior links are not independent random variables drawn from the same population or

Table XXXIV. Link pairs having different length-distribution based on contingency tests.

Contiguous-seven	*Triassic*
Trans-Cis	Trans-Cis
Trans-T	Trans-T
Trans-TB	Trans-TB
Cis-T	
Cis-B	
T-B	T-B
T-TB	
B-TB	
S-TS	S-TS

Table XXXV. Link types of contiguous-seven and Triassic samples arranged in descending order of mean length.

Contiguous-seven		*Triassic*	
Link type	*Mean length (feet)*	*Link type*	*Mean length (feet)*
T	880	TS	1752
TS	827	T	1663
TB	725	TB	1650
Cis	682	S	1454
S	601	Cis	1435
B	553	Trans	1132
Trans	544	B	1118

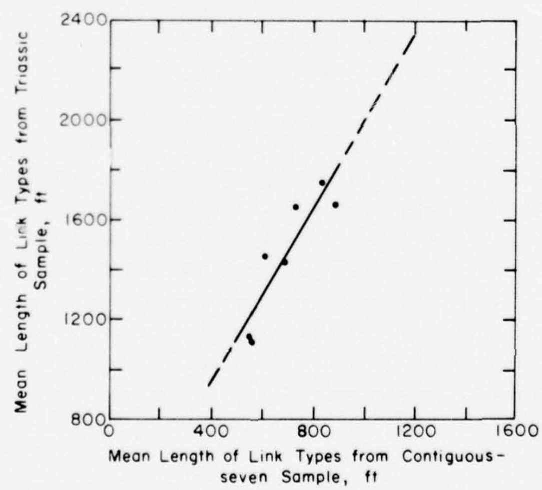

Figure 17. Mean length of each of the seven link types for the Triassic and contiguous-seven samples plotted against each other.

populations. When considered by type, the evidence for a characteristic link length property is stronger in the contiguous-seven sample than in the Triassic streams. This may be of some significance (the Triassic sample being less geologically controlled than the contiguous-seven streams) in light of Werner and Smart's (1973) comment that, in an unpublished study of dendritic networks, they found all interior links had essentially the same link-length distribution with the exception of T-links.

The high correlation between link type and mean length for the two samples suggests that a systematic relationship exists between these variables. It is apparent though that this area of inquiry needs more study, particularly with a more homogeneous set of channel networks.

SUMMARY AND CONCLUSIONS

Introduction

The infinite topologically random model serves as a norm with which the topological properties of real networks can be compared. The model postulates that, in the absence of geologic controls, channel networks will be topologically random. This study examines in detail a sample of channel networks in which the presence of geologic controls is clearly evident from their network patterns. While the stream patterns are striking, their departure from the expectations of topological randomness are much less discernible.

The samples used in this study can be considered as two parts of a continuum which ranges from the classic trellis patterns with a dominance of geologic control to the classic dendritic pattern developed with minimal geologic control. The contiguous-seven sample is representative of the trellis end member of this system, while the Triassic sample lies somewhere in the mid range. In this summary, it is shown that the topological characteristics of the channel networks follow a similar continuum, albeit one which is not nearly so broad or as readily visualized.

Basically, two different methods have been used to analyze the topological properties of the sample networks. The first method was to examine sub-networks within the larger samples, grouping the sub-networks into classes such that their frequency of occurrence could be compared with expected frequencies in topologically random populations. The second method examined individual links, looking at their frequency of occurrence as a function of magnitude, then as a function of type, and finally as a function of type and magnitude.

Sub-networks

All sub-networks ranging in size from magnitude 4 to magnitude 10 within the two samples were examined. At the magnitude-4 level, the networks were grouped into individual TDCN and right-left classes. At higher magnitudes, right-left classes, ambilateral classes, and stream numbers formed the bases for grouping. In all cases, the observed frequencies of occurrence were compared with those expected in a topologically random population. Interpretation of the results from the Triassic streams is quite simple; the hypothesis that these samples were drawn from a topologically random population can be accepted at the 0.05 level except in the one case in which an excessive number of magnitude-10 streams have the stream numbers (10, 2, 1). Considering the number of tests, this constitutes only a small deviation, and the general conclusion that these samples were drawn from a topologically random population is justified.

Apparent geologic controls are discernible in the topological characteristics of the contiguous-seven sample. However, they are subtle and appear to affect only the smallest streams, i.e. the magnitude-4 networks, where there is a preferential development of tributaries entering from the

same side. This excess is most pronounced in those networks whose direction of flow is parallel to the regional strike, indicating a preferential development of tributaries, related to the dip direction. Surprisingly enough, a similar tendency is not apparent in the magnitude-5 networks, although the smaller sample size limits the detail of study. This leads to caution in ascribing geologic controls as a causal mechanism. From magnitude 5 to magnitude 10, all tests indicate no reason to reject the hypothesis that the samples could have been drawn from topologically random populations. Thus, the general conclusion is that, with the exception of magnitude-4 networks, the topologically random model provides the best explanation for the observations.

Links

Analysis of the link structure of networks provides quite a different means of viewing topological characteristics. In this study, analysis of link frequencies as a function of type and magnitude has revealed departures from the expectations of topological randomness that can be related to geological controls.

The contiguous-seven channel networks have a classical trellis drainage pattern. Major channels are approximately parallel to each other and flow along the strike direction. This particular geometry puts a constraint on tributary development, both in the formative stage of the networks and in later adjustments. The parallelism of the main channels and more resistant intervening rocks limits the size to which tributary channel networks can expand. Thus one can expect to find an excess of links in some particular magnitude range depending upon the spacing of master channels, and a deficiency through some higher magnitude range, when compared with the expected frequencies of a topologically random network.

Interior and exterior links form the basic subdivision of links by type. However, in the section *Link Probabilities* (p. 26) both interior and exterior types were further subdivided. The interior-link types can be thought of in terms of their relationship to channel sequences. A channel sequence is terminated downstream with a T-link when it meets an equal- or higher-magnitude sequence, and upstream with a B-link; a link bifurcates into two links of equal magnitude. All the intervening links constitute CT-links. A TB-link is a channel sequence of one link. Thus, for each T-link, there exists exactly one B-link and zero or more CT-links. For finite or infinite topologically random networks, the expected numbers of each type can be specified. If geological controls actively limit random growth, i.e. force development of small networks, then an excess of T- and B-links, and a deficiency of CT-links, can be expected.

The frequency distribution of link magnitudes observed in the contiguous-seven and Triassic streams were compared with the expected frequencies assuming both samples were drawn from an infinite topologically random population. Using a chi-square goodness-of-fit test, there was no reason to reject the hypothesis at the 0.05 level for the Triassic sample. The hypothesis was rejected for the contiguous-seven sample where an excess of magnitude-2 and -3 links, and a dearth of magnitude-5 through -9 links, largely caused the rejection.

The frequency distribution of link types in both samples was compared and tested in the same manner as above with similar results; the Triassic sample could have been drawn from a topologically random population; and the contiguous-seven improbably so. Further testing of the contiguous-seven sample showed that neither the interior-link types nor the exterior-link types, when considered separately, occurred with the frequencies expected if drawn from a topologically random population. Greater than expected frequencies occur in the T, B and TB categories (those links which terminate channel sequences), and a deficiency of CT-links, implying an organization made up of greater than expected short channel sequences.

By combining the frequencies of link type and link magnitude for comparison with expected frequencies, a fairly powerful tool is available for detection of the network structure. As in previous statistical tests, the contiguous-seven networks can be rejected as having been drawn from a topologically random population. Table XXIX reveals in detail where the major departures occur:

1. An excess of magnitude-3 to -5 T-links, i.e. short channel sequences.

2. A deficiency of CT-links (trans and cis) through magnitude 8.

At magnitudes greater than 10, large departures from expected frequencies also occur but, because of the nature of the sample, i.e. complete networks rather than a random sample, less significance can be attributed to those departures. The significance of item 1 above is that geological factors are acting as a partial constraint on network growth, limiting the potential expansion of networks tributary to the master streams, thus resulting in a much larger number of relatively small complete networks than would occur in a topologically random network.

In contrast to the contiguous-seven, the Triassic streams appear to represent a topologically random population.

The classification of link types was based solely on the numerical relationships of each link with its adjoining links at the upstream and downstream junctions. The mean lengths of each link type and their length-frequency distributions were analyzed to determine whether type differences were also reflected in length differences. The results were somewhat ambiguous in that separate length populations did not appear to be present for each link type, while, at the same time, the hypothesis that the individual samples were drawn from a common link-length population could be rejected. The similarity in the trend of mean link length as a function of type, shown by both the Triassic and contiguous-seven samples (Fig. 17), suggests a correlation between link type and link length.

To summarize, the infinite topologically random model of channel networks serves as a comparative base for interpreting topological properties of real channel networks. As a predictor, it is remarkably accurate, to the extent that even a network with strong geologic controls, such as the contiguous-seven sample, shows only subtle departures from topological randomness.

LITERATURE CITED

Abrahams, A.D. (1972) The significance of maximum extension of drainage networks for the frequency distribution of interior link lengths. *Journal of Geology*, vol. 80, p. 730-736.

Army Materiel Command (1972) Engineering Design Handbook. Tables of the Cumulative Binomial Probabilities; AMCP 706-109, 626 p.

Feldman, S., S.A. Harris and R.W. Fairbridge (1968) Drainage patterns. In *Encyclopedia of geomorphology* (R.W. Fairbridge, Ed.). New York: Reinhold Book Corporation, p. 284-291.

Glock, W.S. (1931) The development of drainage systems: a synoptic view. *Geog. Rev.*, vol. 21, p. 475-482.

Horton, R.E. (1932) Drainage basin characteristics. *American Geophysical Union Transactions*, p. 446-460.

Horton, R.E. (1945) Erosional development of streams and their drainage basins; hydrophysical approach to quantitative morphology. *Bull. Geol. Soc. Amer.*, vol. 56, p. 275-370.

James, W.R. and W.C. Krumbein (1969) Frequency distribution of stream link lengths. *Journal of Geology*, vol. 77, p. 544-565.

Krumbein, W.R. and R.L. Shreve (1970) Some statistical properties of dendritic channel networks. Technical Report no. 13, Office of Naval Research Geography Br., Contract Nonr-1228(36), ONR Task No. 389-150 and Special Proj. Rpt. NSF Grant GA-1137, Dept. of Geol., U. of Calif., L.A., 117 p.

Lattman, L. (1968) Structural control in geomorphology. In *Encyclopedia of geomorphology* (R.W. Fairbridge, Ed.). New York: Reinhold Book Corporation, p. 1074-1079.

Leopold, L.B., M.G. Wolman and J.P. Miller (1964) Fluvial processes in geomorphology. W.H. Freeman and Co., San Francisco, 522 p.

Mock, S.J. (1971) A classification of channel links in stream networks. *Water Resources Research*, vol. 7, p. 1558-1566.

Mood, A.M., F.A. Graybill and D.C. Boes (1974) *Introduction to the theory of statistics.* 3rd ed. New York: McGraw-Hill Book Co., 564 p.

Miller, R.L. and J.S. Kahn (1962) *Statistical analysis in the geological sciences.* New York: John Wiley & Sons, Inc., 483 p.

Rao, C.R. (1952) *Advanced statistical methods of biometric research.* New York: John Wiley & Sons, Inc., 390 p.

Schumm, S.A. (1956) Evolution of drainage systems and slopes in badlands at Perth Amboy, N.J. *Bull. Geol. Soc. Amer.*, vol. 67, p. 597-646.

Shreve, R.L. (1966) Statistical law of stream numbers. *Journal of Geology*, vol. 74, p. 17-37.

Shreve, R.L. (1967) Infinite topologically random channel networks. *Journal of Geology*, vol. 75, p. 178-186.

Shreve, R.L. (1969) Stream lengths and basin areas in topologically random channel networks. *Journal of Geology*, vol. 77, p. 397-414.

Smart, J.S. (1968) Statistical properties of stream lengths. *Water Resources Research*, vol. 4, p. 1001-1014.

Smart, J.S. (1969) Topological properties of channel networks. *Bull. Geol. Soc. Amer.*, vol. 80, p. 1757-1774.

Strahler, A.N. (1952) Hypsometric (area-altitude) analysis of erosional topography. *Bull. Geol. Soc. Amer.*, vol. 63, p. 1117-1142.

Strahler, A.N. (1954) Statistical analysis in geomorphic research. *Journal of Geology*, vol. 62, p. 1-25.

Thornbury, W.D. (1954) *Principles of geomorphology.* New York: John Wiley & Sons, Inc., 618 p.

U.S. Geological Survey (1970) The national atlas of the United States of America. U.S. Dept. of Interior, Geological Survey, Wash., D.C., 417 p.

Werner, C. and J.S. Smart (1973) Some new methods of topologic classification of channel networks. *Geogr. Anal.*, vol. 55A, p. 271-295.

Willard, B., J. Freedman, H.B. Roberts, D.B. McLaughlin, L.C. Peltier, H.R. Gault and J.H. Both, Jr. (1959) Geology and mineral resources of Bucks Co., Pennsylvania, Pa. Geol. Survey, Fourth Series, Bulletin C9, 243 p.

Zernitz, E.R. (1932) Drainage patterns and their significance. *Journal of Geology*, vol. 40, p. 498-521.

APPENDIX A. STATISTICAL DATA FOR THE CONTIGUOUS-SEVEN AND TRIASSIC CHANNEL NETWORKS

Stream	*Magnitude*	*Link type*	*Number*	*Mean length (feet)*
Lick Run	117	Trans	34	734
		Cis	31	785
		T	15	867
		B	15	456
		TB	21	958
		S	66	743
		TS	51	930
Barton Hollow	102	Trans	33	435
		Cis	23	525
		T	12	741
		B	12	787
		TB	20	748
		S	56	744
		TS	46	970
Willow Run	380	Trans	117	561
		Cis	81	779
		T	63	1055
		B	63	722
		TB	55	724
		S	218	588
		TS	162	925
George Creek	246	Trans	76	530
		Cis	60	633
		T	38	742
		B	38	603
		TB	33	735
		S	126	610
		TS	120	800
Tuscarora East	385	Trans	93	555
		Cis	114	635
		T	68	831
		B	68	409
		TB	41	545
		S	200	482
		TS	185	700
Tuscarora West	281	Trans	87	516
		Cis	82	706
		T	32	836
		B	32	435
		TB	47	787
		S	150	653
		TS	131	827

Stream	*Magnitude*	*Link type*	*Number*	*Mean length (feet)*
Rhines Hollow	51	Trans	15	363
		Cis	9	569
		T	10	968
		B	10	508
		TB	6	540
		S	28	613
		TS	23	786
Contiguous seven		Trans	455	544
		Cis	401	682
		T	238	880
		B	238	553
		TB	223	725
		S	844	601
		TS	718	827
Stony Brook	274	Trans	73	1095
		Cis	78	1167
		T	46	1875
		B	46	1113
		TB	30	1356
		S	142	1465
		TS	132	1634
Neshanic River	259	Trans	78	997
		Cis	65	946
		T	38	1025
		B	38	885
		TB	39	905
		S	142	991
		TS	117	1446
Tohickon Creek	311	Trans	89	1281
		Cis	110	1914
		T	35	2077
		B	35	1376
		TB	41	2574
		S	148	1885
		TS	163	2068
Triassic		Trans	240	1132
		Cis	253	1435
		T	119	1663
		B	119	1118
		TB	110	1650
		S	432	1454
		TS	412	1752

☆U.S. GOVERNMENT PRINTING OFFICE: 1976–A-0703/95